

Geological Mapping of Lower Indus Basin using Geostatistical and Geophysical Techniques



Nosheen Akhtar
M.Phil (Geophysics)

Department of Earth Sciences
Quaid-i-Azam University
Islamabad, Pakistan

2013-2015

Certificate

It is certified that *Miss Nosheen Akhtar* has carried out the work contained in this dissertation under my supervision and accepted in its present form by Department of Earth Sciences, Quaid-i-Azam University Islamabad and the work fulfills the requirement for award of M.Phil degree in Earth Sciences with Specialization in Geophysics.

RECOMMENDED BY

Supervisor & Chairman:

Dr. M. Gulraiz Akhter

(Chairman

Department of Earth Sciences

Quaid-I-Azam University

Islamabad, Pakistan)

External Examiner:

DEDICATION

To my beloved Niece

Zamal-e-Hoori

*May **ALLAH** keeps HIS special eye on you.*

Acknowledgment

I am extremely grateful to Almighty **ALLAH** who made this universe for His beloved last Prophet **Hazrat Muhammad (S.A.W)**. His (S.A.W) personality is a symbol of kindness and peace for the whole universe till the Day of Judgment. It is bless of ALLAH and prayers of my Parents, which made me able to complete this research work.

I want to acknowledge my thesis supervisor **Dr. M. Gulraiz Akhter**, who has been helpful in guiding me towards the completion of this dissertation. He not only supervised me during my thesis but also thankful for giving his valuable knowledge during the last four years. I am very thankful to the whole faculty members for their valuable time and knowledge.

I have no words to say thanks to **Dr. Khalid Amin khan**, Chief Geophysicist OGDCL/OIST for helping me in the completion of this research work. His knowledge, guidance and valuable comments helped me a lot.

I am very grateful to my beloved parents for believing and supporting me at every stage of my life. **Amma Jee** you are a source of light for me, it is just you who brought up us in very difficult and problematic conditions. You are a role model for all of us. **Abu Jee** you always strengthen me by trusting me and I will never forget your special affection towards me.

I am also very thankful to my brothers specially **Rehan bahi** and sisters for their love, moral support and critical comments. I am very thankful to my very beloved Niece **Zammal-e-Hoori** for making me special and my kid I really love you and always pray for your health and happy life.

I want to say thanks to my university friends specially Ayesha and Aqsa for their moral support and care. I hope this relation will remain evergreen. Last but not least, QAU you thought me a lot about every prospect of life. You brighten my mind and open different ways of thinking. I get a great chance here to understand people. Now I have friends from all area of Pakistan, just because of friendly and peaceful environment of our university. I am very thankful to my department, you made me. I wana say thanks to my fellows, seniors, juniors and departmental staff for their moral support.

Nosheen Akhtar
2015

Table of Contents

List of Figures	viii
List of Tables	x
Abstract	xi
Chapter 1 Introduction	1
1.1 Introduction	2
1.2 Location of the Area.....	2
1.3 Base Map	3
1.4 Data Set	5
1.5 Objectives.....	5
1.6 Methodology	5
1.7 Thesis Outline	6
Chapter 2 Geological Setting.....	7
2.1 Regional Geology	8
2.2 Basins of Pakistan	8
2.3 Geological framework of Lower Indus Basin	9
2.4 Evolution of Lower Indus Basin	9
2.5 Stratigraphic Units	10
2.6 Petroleum Geology	11
Chapter 3 Initial Data and Pre Processing	13
3.1 Pre Processing	14
3.2 Available Data and Data Preparation.....	14
3.3 Selection of Specific Formations.....	16
Chapter 4 Geostatistical Techniques	18
4.1 Introduction.....	19
4.2 Ordinary Kriging.....	19
4.2.1 Variogram	20
4.2.2 Model Variograms	21
4.3 Trend Surfaces Analysis.....	23
4.4 Universal Kriging	24
Chapter 5 Geostatistical Mapping.....	25
5.1 Introduction.....	26

5.2 Kirthar Formation	28
5.2.1 Statistical Analysis of Kirthar Formation	29
5.2.2 Standard Error of Kirthar Formation.....	29
5.2.3. Histogram Analysis of Kirthar Formation	30
5.2.4. 3D surfaces of Kirthar.....	31
5.3 Laki Formation	34
5.3.1 Statistical Analysis of Laki Formation	34
5.3.2 Standard Error of Laki Formation	35
5.3.3 Histograms Analysis of Laki Formation	35
5.3.3 3D surfaces of Laki Formation	36
5.4 Ranikot Group.....	38
5.4.1 Upper Ranikot Formation.....	38
5.4.1.1 Statistical Analysis of Upper Ranikot Formation.....	38
5.4.1.2 Standard Error of Upper Ranikot Formation	39
5.4.1.3. Histogram Analysis of Upper Ranikot.....	39
5.4.1.3 3D Surfaces of Upper Ranikot	40
5.4.2 Lower Ranikot Formation	41
5.4.2.1 Statistical Analysis of Lower Ranikot Formation.....	42
5.4.2. 2 Standard Error of Lower Ranikot Formation	42
5.4.2.3 Histogram Analysis of Lower Ranikot.....	42
5.4.2.3 3D Surfaces of Lower Ranikot	43
5.5 Parh Limestone	44
5.5.1 Statistical Analysis of Parh Limestone.....	45
5.5.2 Standard Error of Parh Limestone	45
5.5.3 Histograms Analysis of Parh Limestone	46
5.5.3 3D Surfaces of Parh Limestone	46
5.6 Goru Formation.....	48
5.6.1 Upper Goru	49
5.6.1.1 Statistical Analysis of Upper Goru.....	49
5.6.1.2 Standard Error of Upper Goru	49
5.6.1.3 Histogram Analysis of Upper Goru.....	50
5.6.1.4 3D Surfaces of Upper Goru	50

5.6.2 Lower Goru Formation	53
5.6.2.1 Statistical Analysis of Lower Goru	53
5.6.2.2 Standard Error of Lower Goru	53
5.6.2.3 Histogram Analysis of Lower Goru	54
5.6.2.3 3D Surfaces of Lower Goru	54
5.7 Chiltan Formation	56
5.7.1 Statistical Analysis of Chiltan Formation	56
5.7.2 Standard Error of Chiltan Formation	56
5.7.3 Histogram Analysis of Chiltan	57
5.7.4 3D surfaces of Chiltan Formation	58
Chapter 6 Digital Sub-Surface Model	60
6.1 Introduction	61
6.2 Development of Digital Sub Surface Model	61
6.3 Software Application	61
6.4 Bilinear Interpolation	63
6.5 Practical Application	64
6.5 2D synthetic seismic model	69
6.6 Seismic Line PK-92	74
Conclusion and Recommendations	75
Conclusions	76
Recommendations	76
References	77
Appendix 1	79

List of Figures

Fig 1.1: Location Map of Study Area.....	3
Fig 1.2: Base map of study area	4
Fig 2.1: Sedimentary Basins of Pakistan.....	9
Fig 2.2: Tectonic map of Pakistan showing geological setting of study area.....	10
Fig 2.3: Stratigraphic chart of lower Indus basin.....	12
Fig 3.1 Generalized flow chart of data preparation.	14
Fig 3.2: Initial Format of Data.	15
Fig 3.3: Data in Record Form.	15
Fig 3.4: Total records found for selected formation Upper Goru.	16
Fig 4.1: Application/working of search radius method.	20
Fig 4.2: Model Variogram indicating the Nugget, Sill and Range.....	21
Fig 4.3: Model Variograms.....	21
Fig 4.4: Experimental Variogram approximated with Model Variogram.....	22
Fig 4.5: Procedure to construct trend surface polynomial equations of order 1 to 3.....	23
Fig 5.1: Geostatistical Gridding and Analysis Workflow.....	27
Fig 5.2: User Interface of K-tron GridWorks used for Geostatistical Modeling.....	28
Fig 5.3: Histograms of XYZ data (A), XYZ Filtered data (B), Ordinary Kriging (C) and Universal Kriging (D).	31
Fig 5.4: 3D Surfaces of Kirthar Formation.....	33
Fig 5.5: Histograms of Laki Formation of XYZ (A) and XYZ filtered data (B)	35
Fig 5.6: 3D Surfaces of Laki Formation.....	37
Fig 5.7: Histograms of XYZ (A) and XYZ filtered data (B) of Upper Ranikot.....	39
Fig 5.8: 3D surfaces of Upper Ranikot.....	41
Fig 5.9: Histogram of XYZ (A) and filtered XYZ data (B) of Lower Ranikot.....	43
Fig 5.10: 3D Surfaces of Lower Ranikot.....	44
Fig 5.11: Histogram of XYZ (A) and filtered XYZ data (B) of Parh.....	46
Fig: 5.12: 3D Surfaces of Parh Limestone.....	48
Fig 5.13: Histogram of XYZ and XYZ filtered data of Upper Goru	50
Fig 5.14: 3D surfaces of Upper Goru.....	52
Fig 5.15: Histograms of XYZ (A) and XYZ filtered data (B) of Lower Goru.....	54

Fig 5.16: 3D surfaces of Lower Goru.....	55
Fig 5.17: Histograms of XYZ (A) and XYZ filtered data (B) of Chiltan Formation.....	57
Fig 5.18: 3D surfaces of Chiltan Formation.....	59
Fig 6.1: The interface of GridWorks: Digital Sub-Surface Model application.....	62
Fig 6.2: Workflow of Columns and Cross-Section generation.....	62
Fig 6.3: Column generation interface	63
Fig 6.4: Linear Interpolation at point P.....	64
Fig 6.5: Individual Grid Nodes of Upper Ranikot Formation.....	65
Fig 6.6: Grid nodes for all formations central part is overlapping zone.....	65
Fig 6.7: Selection of spatial location and all formations present beneath that point.....	66
Fig 6.8: Generation of 1D column at geographic location C8.....	66
Fig. 6.9: Columns generated for eight locations (C1-C8) along all the encountered formations	67
Fig 6.10: DSSM which interactively marked lines.....	68
Fig 6.11: The cross section generated from line S1.....	69
Fig 6.12: 2D Synthetic Seismic Model of S1.....	69
Fig 6.13: The cross section generated from line S2.....	70
Fig 6.14: 2D Synthetic Seismic Model of S2.....	70
Fig 6.15: The cross section generated from line S3.....	71
Fig 6.16: 2D Synthetic Seismic Model of S3.....	71
Fig 6.17: The cross section generated from line S4.....	72
Fig 6.18: 2D Synthetic Seismic Model of S4.....	72
Fig 6.19: The cross section generated from line S5.....	73
Fig 6.20: 2D Synthetic Seismic Model of S5.....	73
Fig 6.21: Interpreted PK-92 with Digital sub Surface Model	74
Fig 6.22: Interpreted PK-92 with Digital sub Surface Model zoomed section.....	74

List of Tables

Table 1: Selected formations with total records and average formation's top.	17
Table2: Statistical Analysis of Kirthar Formation.	29
Table3: Standard Error of Kirthar Formation.	30
Table 4: Statistical Analysis of Laki Formation.	34
Table 5: Standard Error of Laki Formation.	35
Table 6: Statistical Analysis of Upper Ranikot.	38
Table 7: Standard Error of Upper Ranikot.	39
Table 8: Statistical Analysis of Lower Ranikot.	42
Table 9: Standard Error of Lower Ranikot.	42
Table 10: Statistical Analysis of Parh Limestone.	45
Table 11: Standard Error of Parh Limestone.	45
Table 12: Statistical Analysis of Upper Goru.	49
Table 13: Standard Error of Upper Goru.	50
Table 14: Statistical Analysis of Lower Goru.	53
Table 15: Standard Error of Lower Goru.	53
Table 16: Statistical Analysis of Chiltan Formation.	56
Table17: Standard Error of Chiltan Formation.	57

Abstract

For a number of years regional studies are in progress to understand the structural and tectonic features of different stratigraphic units of a basin. Ordinary Kriging, Trend Surface analysis and Universal Kriging techniques are used to analyze and model the topographic variations of sedimentary cover of Lower Indus Basin. The input data used for this process is formation top of 461 wells. Statistical analysis is carried out on the data to estimate variance and standard error between the generalized model surfaces. Surfaces of different formations are generated by using Ordinary Kriging, Trend surface analysis and Universal Kriging techniques. Ordinary Kriging gives more detail in terms of local variations while Universal Kriging provides the regional trend. Trend surface analysis uses polynomial regression of increasing order up to 3. Surfaces of high orders are generated to effectively account the variation in formation tops. But surfaces of high orders cannot be generated due to complex geometry problems. Initially Universal Kriging was selected as final technique on the bases of standard deviation and standard error value, but after some tests it was found that Ordinary Kriging along with a smoothing operator of very high order produces similar results. To compromise between localized and regional trends Ordinary Kriging along with smoothing kernel operator of 21×21 points. The Geostatistical grids are used to assemble a multilayer Digital Sub-Surface Model (DSSM) which can be used to generate columns and subsurface cross-sections within the area at any location within the geographic window. This can be useful in seismic interpretation of adjacent areas, establishing well control over a point and generation of correlation profiles. 2D synthetic seismic models confirm the digital sub-surface models.

Chapter 1 Introduction

1.1 Introduction

For a number of years regional studies are in progress to understand the structural and tectonic features of different stratigraphic units of a basin (Agarwal and Kanasevich, 1971). These studies are very helpful to map the spatial temporal variations in structural and stratigraphic behavior of rock units (Merriam and Harbaugh, 1963; Merriam and Lippert, 1966). In geosciences, data is gathered at some geo referenced location on earth's surface. Data have three coordinates "x" and "y" is the geographic location and "z" is the parameter to map. In some cases we are concerned to map or model the space based variations of one or more parameters, called as spatial variations. In certain cases we are also interested to see space & time based variation of parameters called as spatiotemporal. Analytical methods used to map these trends were Gravity and Magnetic Method data is collected of a large area.

Geostatistics is a branch of statistics focusing on spatial or spatiotemporal datasets. In the current study Ordinary Kriging, Trend Surface Analysis and Universal Kriging are used. Ordinary Kriging is gridding method which uses different variograms and data search criteria for interpolation. Trend surface is a mathematical technique used to compute 2D "plane" or 3D "curves" by using polynomial regression. It is used to separate the data into two components; the regional trend and the local fluctuations called as residuals. It is used to define large scale trends, patterns and provide general structure of spatial variation in large datasets. Universal Kriging uses all data points and gives regional trend.

1.2 Location of the Area

The study area is lower Indus Basin, subdivision of Indus Basin, Pakistan. It is bounded by 68°22'00" to 69°00'35" longitude and 24°18'00" to 25°31'15" latitude. Jacobabad Khairpur High and Mari Khandkot High is the Northern boundary and Indus Offshore is the southern geological boundary of lower Indus basin. While Indian shield bounds it from east and Khirthar fold belt is in the west. The location of study area is shown in map Fig 1.1.



Fig 1.1: Location Map of Study Area (Khan et al., 2008)

1.3 Base Map

Base map of study area is also shown in Fig 1.2 along with its scale. It gives geographic location of 461 wells used in this study. The geographic location of well is very important for mapping different formations of the basin. Exploration, Appraisal and Development wells are included in this study. Bari, Kadanwari, Maino, Tando Alam, Khaskeli, Sui field are main oil/gas fields located in Lower Indus Basin. These fields have both structural and Stratigraphic traps. Lower Goru sandstone of Early Cretaceous age is economically very important.

Lower Indus basin is selected for this study because it is least structurally disturbed area as compared to other basins of Pakistan. Exploration activities and number of wells in this basin is also much high so mapping or correlation will be more easy and accurate.

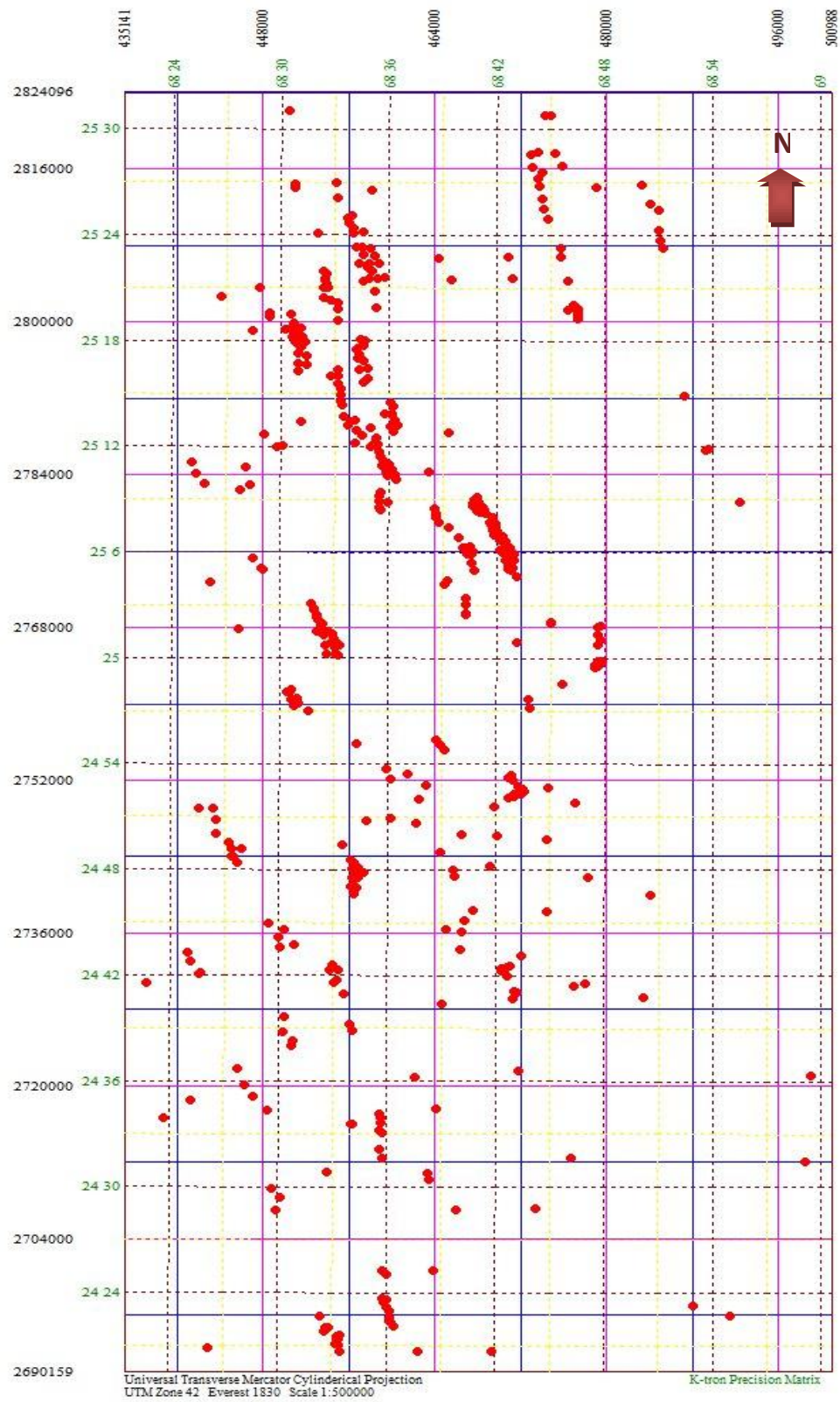


Fig 1.2: Base map of study area (Khan, 2000)

1.4 Data Set

To map the subsurface formations of lower Indus basin, data of 461 wells is obtained from OIST exploration department. The data set consist of formation tops of all these wells. The selected formations are mapped by using Geostatistical techniques such as Ordinary Kriging, Trend Surface analysis, Universal Kriging and Smooth Ordinary Kriging.

1.5 Objectives

1. The prime objective is to model formations of lower Indus basin using Geostatistical Techniques.
2. The Geostatistical grids are used to assemble a multilayer Digital Sub-Surface Model (DSSM). This model can be used:
 - a) To generate 2D contour maps, 3D surfaces, 1D column and 2D cross sections.
 - b) That gives variation in depth of selected formations through 3D surfaces and thickness by 1D column and cross sections.
 - c) These columns and cross sections are useful in seismic interpretation of adjacent areas, establishing well control over a point and generation of correlation profiles.
3. Geological surface have been generated by using different Geostatistical techniques to analyze the local details along with generalized trend.

1.6 Methodology

To map the selected stratigraphic units of lower Indus basin, formation tops of 461 wells is used. Chiltan, Lower Goru, Upper Goru, Parh, Ranikot, Laki, Khirthar Formation are selected for analysis and modeling. These formations were selected on the basis of their continuity in each well and economic value. Such as Goru Formation is a complete petroleum play. Ranikot is acting as source and seal.

The data from the database is initially formatted into a record structure using Visual OIL programs. The final data is input to GridWorks software for Geostatistical analysis and model generation. The raw data is filtered to remove any large spikes and flucations. The filtered data is used to compute model grids using Ordinary Kriging, Trend surface and Universal Kriging algorithms.

Statistical analysis of raw data and each gridded datasets are also carried out to understand the spatial variations. After analysis Universal Kriging has been selected as a final technique to generate the subsurface grid model. Later on it is found that Universal Kriging surface is also

representing the regional trend and gradient of formation throughout the basin. After many tests it is concluded that the surfaces by Ordinary Kriging on smoothing (high orders) are similar to surfaces by Universal Kriging. Thus to generate regional trend along prominent topographic variations Kernel Operator of different orders is tested on Ordinary Kriging. Thus by adjusting smoothing Kernel Operator of 21*21 points Ordinary Kriging is converted into a surface (Smooth Ordinary Kriging), which represents the regional trend and prominent local topographic variations.

The interface of Digital Sub-Surface Model (DSSM) is generated which consists on multiple grids as there are multiple layers are present in subsurface. K-tron GridWorks is a DSSM technology used to create the subsurface model of the area by integrating all the surfaces. Through this technique we can interactively generate 1D subsurface columns and 2D cross sections at any given geographic coordinates.

1.7 Thesis Outline

1st unit is about the brief introduction of study area, data set, objectives and methodology. 2nd is briefly related with geological setting, stratigraphy and petroleum play of the basin. 3rd unit is preparation and filtration of data, which include two Visual OIL programs WellRec.ifc and WellRecF.ifc. 4th unit include general information about Geostatistical techniques used Ordinary Kriging, Trend Surface Analysis and Universal Kriging. 5th unit is about the development of different polynomial equations, 3D surfaces of selected formations by different Geostatistical techniques i.e. Ordinary Kriging, Trend Surface Analysis and Universal Kriging and Smooth Ordinary Kriging of formations. 6th unit is the generalized model of selected formations and development of a computer interface to model formations of lower Indus basin. 7th unit is about the conclusions and recommendations.

Chapter 2 Geological Setting

2.1 Regional Geology

Indian Plate separated from Gondwanaland and migrated northwards during early to middle Cretaceous (Powell and Conaghan 1973). Laurasian, Tethyan and Gondwanaland domains are geological subdivisions of Pakistan from North to South (Kazmi and Jan, 1997). The origin of these domains may be back to Late Paleozoic. Earlier there was a super continent called as Pangaea, but in late Triassic Pangea split into two large landmasses i.e. Laurasia to the north and Gondwanaland to the south separated by the Tethys seaway. Pakistan is located at the junction of Gondwanian and Tethyan domains.

2.2 Basins of Pakistan

Indus basin, Baluchistan basin and Pishin basin are three sedimentary basins of Pakistan (Kadri, 1995). Indus basin is more explored and its subdivision is as under; (Kemal et al., 1991).

- i. Upper Indus Basin**
- ii. Middle Indus Basin**
- iii. Lower Indus Basin**

Middle Indus Basin is separated in North from upper indus basin by Sargodha Highs and in South from lower Indus basin by Jacobabad-Mari-Kandkot High as shown in Fig 2.1. The main focus of this study is Lower Indus basin.

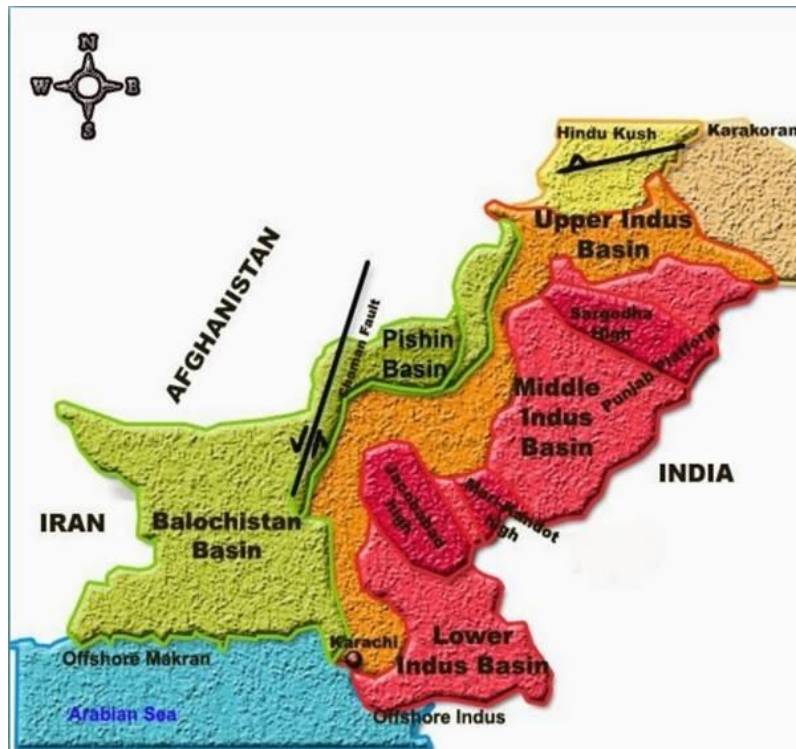


Fig 2.1: Sedimentary Basins of Pakistan (Kemal et al., 1991).

2.3 Geological framework of Lower Indus Basin

Lower Indus basin is separated from central Indus basin in the north by a positive feature that is Mari Kandkot high. It extends to the offshore in the south. While Indian shield is in east and Kirthar fold belt is in the west. There are five main units of the basin, which are given as below; (Kazmi and Jan, 1995).

1. Thar Platform
2. Kirthar Fore deep
3. Kirthar Fold belt
4. Karachi Trough
5. Offshore Indus

2.4 Evolution of Lower Indus Basin

Margins of Lower Indus basin are mainly affected by rifting between India and Madagascar. (Zaigham and Mallick, 2000) proposed a structural model, which leads following conclusions about evolution of basin.

1. The first step of structural model is about the occurrence of divergent phenomena because rifting of Gondwanaland in Paleozoic. That results magma formation in Asthenosphere and structural disturbance i.e. stretching and Normal faulting in lithosphere. The process of sea floor spreading began with basaltic magma upwelling to the earth surface at oceanic Lithosphere.
2. In second step active faults that turn the brittle crust into blocks during active sea floor spreading. Then at some geological time, stretching stops and that stretched part of crust act as Indus basin.
3. The third step is about the accumulation of sediments of Mesozoic and Tertiary age in basin. Thick Sediments of different geologic ages are exposed at different locations of Indus basin.

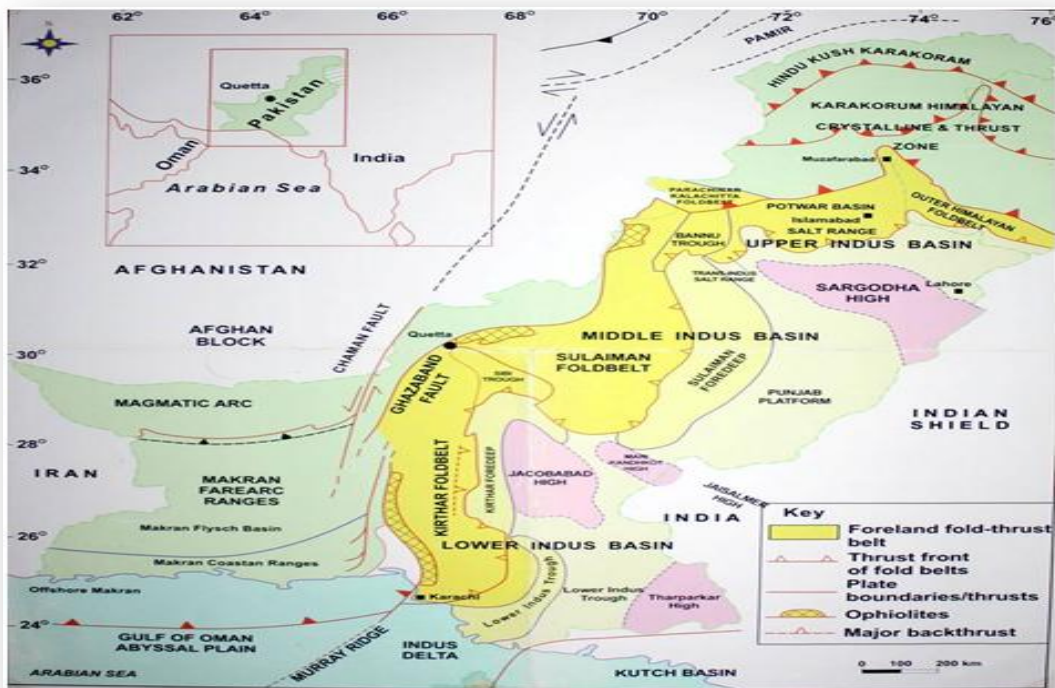


Fig 2.2: Tectonic map of Pakistan

2.5 Stratigraphic Units

Stratigraphy of the study area ranges from Triassic to Holocene. The sound knowledge of stratigraphic settings of basin is very useful for hydrocarbon prospecting. It is very helpful in understanding trapping mechanisms and depositional environment of the rocks in a basin.

In the southeastern part of the basin basement (Precambrian) is exposed. Two Important unconformities are present, one at base Permian and the other at base Tertiary. The sediments of the lower Indus basin are thick westward. Stratigraphic succession of lower Indus basin changes from east to west. The stratigraphy of study area (Kadri, 1995) is shown in Fig 2.3.

2.6 Petroleum Geology

Petroleum generation is time and space dependant process. Hydrocarbons are generated in organic rich source rock at controlled temperature and pressure, followed by migration in porous and permeable reservoir rock. Hydrocarbon fluids will continue migration until trapped and covered by impermeable seal rock. This process will take millions of years.

According to petroleum system of lower Indus basin, early Cretaceous rocks i.e. Sember and Lower Goru are source rock. Cretaceous to Eocene clastics and carbonates are reservoirs i.e. Lower Goru, Ranikot, Sui Main Limestone and Habib Rahi Formation. Intra-formational shale of Goru Formation and Ghazij Formation are acting as seal rocks in basin. Both Structural and Stratigraphic traps are present. Structural trapping mechanism in the Lower Indus Basin consists on tilted fault blocks and faulted gentle role-overs.

ERA	PERIOD	EPOCH	INDUS BASIN											
			UPPER					SOUTHERN/CENTRAL						
			SUB BASIN/FORMATION					BASIN/FORMATION						
			POTWAR		KOHAT			KIRTHAR		SULAIMAN				
Cenozoic	QUATERNARY	PIEISTOCENE	LEI Conglomerate					LEI Conglomerate						
		TERTIARY	PLIOCENE	SIWALKS GROUP	SOAN (cl, sst)			SIWALKS GROUP (sst)						
	DHOK PATHAN (CL, SST)													
	MIOCENE		NAGRI (SST)			GAJ FORMATION (sst, sh, ls)								
			CHINJI (SST, SH)											
	PALEOCENE		RAWALPINDI GROUP		KAMLIJAL (SST)									
					MURREE (sst, cl)									
	TERTIARY	OLIGOCENE						NARI FORMATION (ls, sst)						
		EOCENE	CHHART GROUP				KIRTHAR FM (ls)		KIRTHAR FORMATION	DARZIDA MEMBER (cl)				
							KUL DANA (cl)			PIRKOH MEMBER (ls)				
				CHOR GALLI (ls, mrl)			JATTA GYP (gyp, sh)			DOMANDA MEMBER (CL)				
				SAKESAR (ls)			SHEKHAN (ls)			HABIB RAHI FM (ls)				
		PALEOCENE		NAMMAL (ls, mrl)			RANOBA (sh)		BAHOUR RHEL SALT		BASKA SHALE (sh)			
							PATJALA FM (sh, ls)			LAKHI FM (ls)		GHAZI FM (sh)		
							LOCHART Lst (ls)			LAKHRA FM (ls, sh)		DUNGHAN FM (ls)		
							HANGU FM (sst)			BARA FM		RANIKOT (sst, sh)		
							KHADRO FM (sst)			SUI MAIN LIMESTONE (ls)				
Mesozoic	CRETACEOUS	LATE				KAWAGARH (ls)		PAB SANDSTONE (sst)						
							FORT MUNRO MEMBER (ls, mrl)							
	EARLY				LUMSHI WAL (sst, silt, st)		MOGHALKOT FM (sst, ls, sh)							
							TARH FORMATION (ls)							
	JURASSIC	LATE				CHICHALI (silt, st, cl)		GORU FORMATION (sst, sh)						
		MIDDLE				?		SEMIAR FORMATION (silt, st, sh)						
		EARLY	SAMANA SUK FM (ls)			MAZAR DRIK (sh)								
	SHINWARI FM (sst, ls, sh)			CHILIAN FORMATION (ls)										
	TRIASSIC	LATE				DAITA FM (sh)		SHIRINAB FORMATION (ss, ls)						
		MIDDLE				?								
		EARLY						WULGAI FORMATION (sst, sh, ls)						
Paleozoic	PERMIAN	LATE	ZALUCH GROUP	CHIHIDRU FM (sst, ls)					NOT EXPOSED OR DRILLED					
		WARGAL (ls)												
		EARLY	NEUWAN GROUP	AMB FM (sst, ls)										
				SARDHAI FM (cl)										
				WAR CHIBIA FM (sst)										
				DANDOT FM (cl, sst)										
	TOBRA FM (sst, cong)													
	CARBONIFE TO ORDOVICIAN													
	CAMBRIAN	LATE												
		MIDDLE	JHELM GROUP	BAGHANWALA FM (sh)		KHISOR FM (gyp, anh, sh)								
		JUTANA FM (dol)												
			EARLY			KUSSAK (sst, silt, st)								
						KHEWRA SANDSTONE								
PRE-CAMBRIAN			SAIT RANG F FM (silt, gyp, anh)											

Fig 2.3: Stratigraphic chart of lower Indus basin (after Kadri, 1995).

Chapter 3 Initial Data and Pre Processing

3.1 Pre Processing

OGDCL/OIST exploration department has been used as a source for data. The data is in geographic window 68° 22' 00" to 68°36'67" latitude and 69° 00' 35" to 69°00'97" is extracted. The database system provides the data in report form. For current analysis the data needs to be formatted in a record structure. So that it will be easy to filter out data for any specific formation. For this purpose two Visual OIL programs WellRec.ifc and WellRecF.ifc (Appendix 1) have been utilized. The flow chart of this process is shown in Fig 3.1.

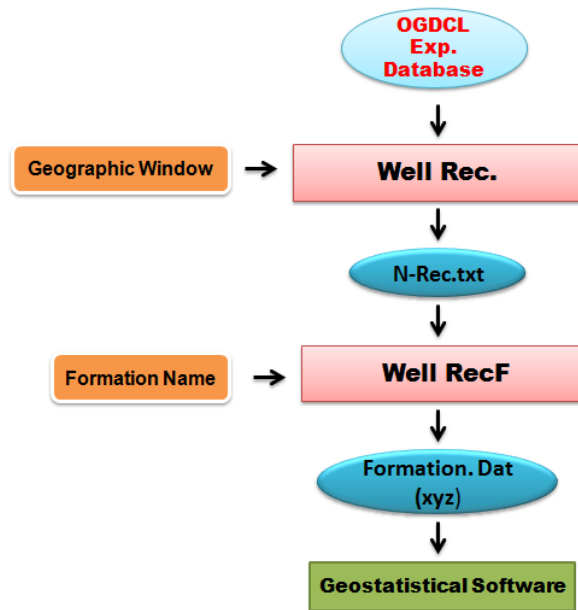


Fig 3.1: Generalized flow chart of data preparation.

3.2 Available Data and Data Preparation

For current study, the available data is in report form. It contains header and formations encountered in those wells. To map the selected formations, the data needs to be formatted in a record structure. So that it will be easy to filter out data for any specific formation. For this purpose two Visual OIL programs WellRec.ifc and WellRecF.ifc (Appendix1) have been utilized. The initial format of data is given in Fig 3.2.

```

Nosheen-H.I.XI - Notepad
File Edit Format View Help
-----
SANDS BELOW TALHAR SHALE 2938.129
-----
Well Name: UNAR_01
-----
Long: 68.572298 Lat: 25.373697
K.B. Elevation: 28.87
Total Depth: 4100
Type: EX
Status: GAS/CON
Operator: OGDCL
Concession: TANDO ALLAH YAR (2568-8)
-----
ALLUVIUM 0
LAKI 70
RANIKOT 616
KHADRO 950
PARH 1063
UPPER GORU 1150
LOWER GORU 2080
A SAND 2080
TURK SHALE 2101
B SAND 2104
BADIN SHALE 2192
C SAND 2255
UPPER SHALE 2331
MIDDLE SAND 2505
LOWER SHALE 2682
BASAL SAND 2792
TALHAR SHALE 2851
MASSIVE SANDS 2911
SEMBAR 3298
CHILTAN LIMESTONE 3889.5
-----
Well Name: WAKU_01
-----
Long: 68.445289 Lat: 25.342167
K.B. Elevation: 21.11
Total Depth: 2550

```

Fig 3.2: Initial Format of Data.

The first program WellRec.ifc (Appendix1) extracts the data in record form within the area of interest containing data of all formations. This data contain all information (corresponding well name, longitude and latitude, K.B elevation, Total depth, type, status, operator and about the concession area) of against every formation that is encountered in all 461 wells of study area, as shown in Fig 3.3.

Well Name	Long	Lat	K.B. Elevation	Total Depth	Type	Status	Operator	Concession	Formation	Depth
ABRI_01	68.583719	25.442642	0.00	2745.00	EX	ABD	OGDCL	TANDO ALLAH YAR (2568-8)	ALLUVIUM	
ABRI_01	68.583719	25.442642	0.00	2745.00	EX	ABD	OGDCL	TANDO ALLAH YAR (2568-8)	LAKI	71.000
ABRI_01	68.583719	25.442642	0.00	2745.00	EX	ABD	OGDCL	TANDO ALLAH YAR (2568-8)	RANIKOT	
ABRI_01	68.583719	25.442642	0.00	2745.00	EX	ABD	OGDCL	TANDO ALLAH YAR (2568-8)	KHADRO	
ABRI_01	68.583719	25.442642	0.00	2745.00	EX	ABD	OGDCL	TANDO ALLAH YAR (2568-8)	PARH	
ABRI_01	68.583719	25.442642	0.00	2745.00	EX	ABD	OGDCL	TANDO ALLAH YAR (2568-8)	UPPER GORU	
ABRI_01	68.583719	25.442642	0.00	2745.00	EX	ABD	OGDCL	TANDO ALLAH YAR (2568-8)	LOWER GORU	
AKAI_01	68.746700	24.761178	18.89	1097.20	EX	ABD	UTP	BADIN-I	KIRTHAR UNDIFF.	76.196
AKAI_01	68.746700	24.761178	18.89	1097.20	EX	ABD	UTP	BADIN-I	RANIKOT	204.511
AKAI_01	68.746700	24.761178	18.89	1097.20	EX	ABD	UTP	BADIN-I	DECCAN TRAP	463.883
AKAI_01	68.746700	24.761178	18.89	1097.20	EX	ABD	UTP	BADIN-I	PARH	518.135
AKAI_01	68.746700	24.761178	18.89	1097.20	EX	ABD	UTP	BADIN-I	UPPER GORU	521.792
AKAI_01	68.746700	24.761178	18.89	1097.20	EX	ABD	UTP	BADIN-I	LOWER GORU	913.136
AKAI_01	68.746700	24.761178	18.89	1097.20	EX	ABD	UTP	BADIN-I	ALLUVIUM	0.000
AKRI_01	68.596186	24.527783	10.36	1801.30	EX	ABD	UTP	BADIN-I	SIWALIK	76.806
AKRI_01	68.596186	24.527783	10.36	1801.30	EX	ABD	UTP	BADIN-I	KIRTHAR EQUIVALENT	152.393
AKRI_01	68.596186	24.527783	10.36	1801.30	EX	ABD	UTP	BADIN-I	GHAZI	291.984
AKRI_01	68.596186	24.527783	10.36	1801.30	EX	ABD	UTP	BADIN-I	RANIKOT	333.435
AKRI_01	68.596186	24.527783	10.36	1801.30	EX	ABD	UTP	BADIN-I	DECCAN TRAP	601.646
AKRI_01	68.596186	24.527783	10.36	1801.30	EX	ABD	UTP	BADIN-I	UPPER GORU	638.220
AKRI_01	68.596186	24.527783	10.36	1801.30	EX	ABD	UTP	BADIN-I	LOWER GORU	1635.477
AKRI_01	68.596186	24.527783	10.36	1801.30	EX	ABD	UTP	BADIN-I	ALLUVIUM	0.000
ALI ZAUR_01	68.554802	25.012708	21.33	2093.00	EX	OIL	BP	BADIN-III (2468-2)	ALLUVIUM-NARI (UNDI)	

Fig 3.3: Data in Record Form.

The second program WellRecF.iff takes the output of previous program and output xyz data for any specific formation.

Now from the output of first program, data of a particular formation from all wells can easily be extracted. For this purpose a second program WellRecF.iff is used that takes the output of previous program as an input. Then XYZ files for particular formations are generated by using Visual OIL (Khan et al., 2010). This program will search the required formation and also gives total number of records i.e. in how many wells that particular formation is encountered. For example data of Upper Goru is extracted. When the search completes it give total records founds that is 398 records as shown in Fig 3.4. On the similar ways, data of other selected formations is extracted and note down the total records found and average top of that formation. This data is then used for Geostatistical analysis.

Well ID	X	Y	Formation	Value
ZAUR_10	25.014576	726.913	UPPER GORU	68.552568
ZAUR_11	25.022855	737.58	UPPER GORU	68.548523
ZAUR_12	25.033161	757.391	UPPER GORU	68.53936
ZAUR_14	25.025931	743.066	UPPER GORU	68.543925
ZAUR DEEP_01	25.012181	744.285	UPPER GORU	68.541416
ZAUR DEEP_02	25.004536	725.389	UPPER GORU	68.542925
ZAUR DEEP_03	25.025797	734.532	UPPER GORU	68.540497
ZAUR SOUTH_01	25.002926	685.767	UPPER GORU	68.553991
ZAUR WEST_01	25.02525	774.764	UPPER GORU	68.533893
ZAUR WIM_13	25.045798	804.633	UPPER GORU	68.531062

Search Completed
398 Records Found.

Fig 3.4: Total records found for selected formation Upper Goru.

3.3 Selection of Specific Formations

These formations were selected based on their economic importance and also these are found in most wells. Such as Lower Goru is a complete petroleum play and total records for this formation are 396. Ranikot is good reservoir. Specific formations which will be mapped are in Table1;

Sr.#	Formation	Records	Lithology	Avg. Formation Top (M)
1.	Kirthar	221	Mainly carbonates	110.5
2.	Laki	117	carbonates	118.6
3.	Upper Ranikot	370	Limestone, sandstone	154
4.	Lower Ranikot	246	Shale, sandstone	317.79
5.	Parh	311	limestone	746.67
6.	Upper Goru	398	shales	824.98
7.	Lower Goru	396	Shale	1719.43
8.	Chiltan	18	Limestone	3194

Table 1: Selected formations with total records and average formation's top.

This data is then used for Geostatistical analysis, and for generation of maps and 3D surfaces of specific formations and GRD files of particular formation is needed to map it. For the generation of grid of every formation the required data is X (Longitude), Y (Latitude) and Z (Top of that formation in different wells). XYZ files are used to extract the required data of these formations, which are planned to map.

Chapter 4 Geostatistical Techniques

4.1 Introduction

Geostatistics is a branch of statistics focusing on spatial or spatiotemporal datasets. In geosciences, data is collected at some geo referenced location on earth's surface. In some cases we are concerned to map or model the space based variations of one or more parameters, called as spatial variations. In certain cases we are also interested to see space & time based variation of parameters called as spatiotemporal variations. Geostatistical algorithms are used for modeling, spatial mapping and analysis of data by all contouring software and geographic information systems (GIS). Three techniques are used for Geostatistical analysis i.e. Kriging, Universal Kriging and Trend Surfaces Analysis for Geostatistical analysis in this study. A brief theory of these techniques is discussed in this chapter.

4.2 Ordinary Kriging

Ordinary Kriging is a weighted moving average technique; it uses different weighting functions depending on the distance and orientation of sample points with respect to the node, and the manner in which sample points are clustered (Khan, 2014).

Ordinary Kriging is a gridding method which uses radius based search method for interpolation. In this method a radius around the grid node and uses all the data points that fall within the given radius for interpolation at the grid node. The radius will be fixed, but number of data points at each grid node may vary. If dataset is dense, then number of data points lying in radius will be high. If there is no data point in that radius then null value will be assigned and interpolation is not carried out. For node A, no sample is found, therefore it is assigned null value, for node B five samples are found and for node C seven samples are found as shown in Fig 4.1. It gives the localized trend of mapped parameter.

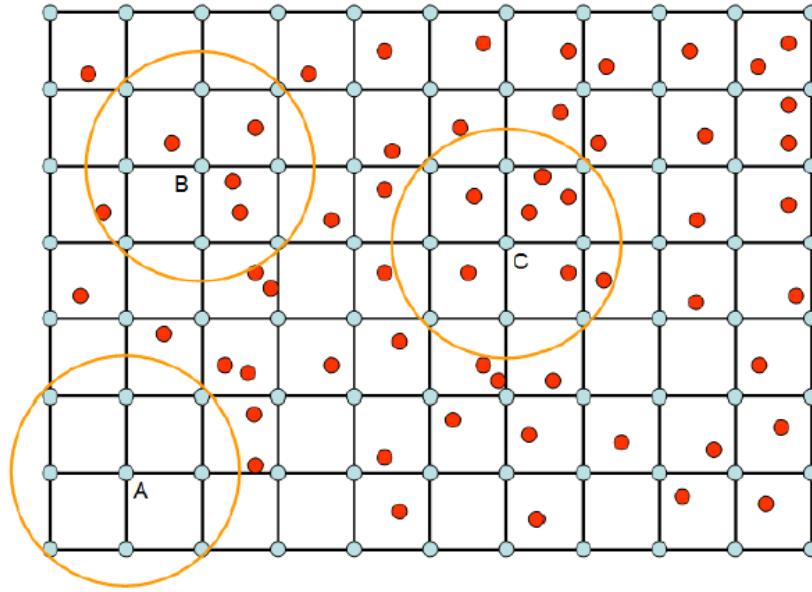


Fig 4.1: Application/working of search radius method (Khan, 2014).

Thus Ordinary Kriging is based on statistical relationship or dependence among the measured points and is determined through estimation of variogram and covariance functions which depict the spatial autocorrelation of the measured data points.

4.2.1 Variogram

Variogram is a function, which is used to derive weighting functions for interpolation in Kriging. The variogram characterizes the spatial continuity or roughness of a data set. It is defined as the variance of the difference between data values at two locations across realizations of the field. Thus it mathematically specifies the variability of the measured data points (Chiles and Delfiner, 2012).

A model variogram is shown in Fig 4.2. It can be seen that at a certain distance, the model levels out. The distance where the model first flattens out is known as the range. The value that the variogram model attains at the range is called the sill. In theory, at zero separation distance (lag = 0), the variogram value is 0. However, at very small separation distance, the variogram often exhibits a nugget effect, which is some value greater than 0. The partial sill is the sill minus the nugget. The nugget effect can be attributed to measurement errors or spatial sources of variation at distances smaller than the sampling interval or both.

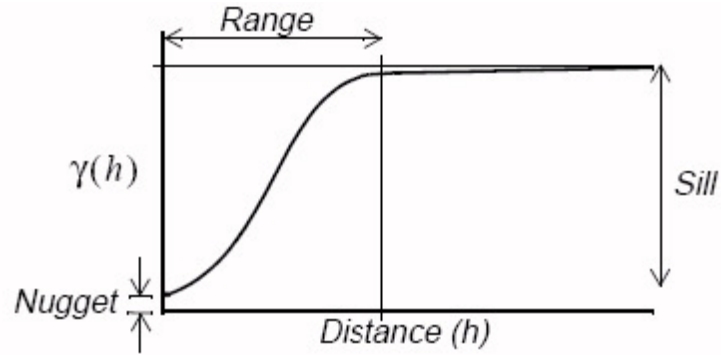


Fig 4.2: Model Variogram indicating the Nugget, Sill and Range

4.2.2 Model Variograms

Mathematically a large number of model variograms have been derived (Cressie, 1985). Some commonly used model variograms are Linear, Quadratic and Gaussian are shown in Fig 4.3.

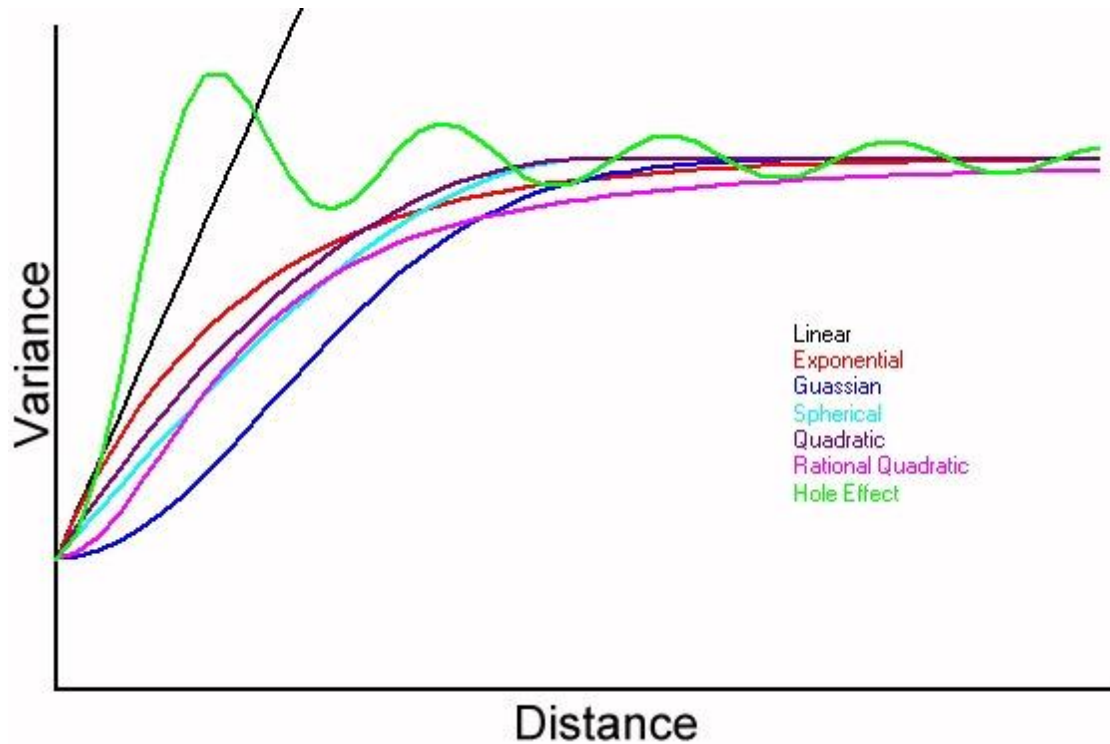


Fig 4.3: Model Variograms

Mathematical expressions for some model variograms are given, when \mathbf{h} is the distance, \mathbf{r} is the range and \mathbf{C} (Nugget + Partial Sill) is the scale.

Exponential Variogram Model

$$\gamma(h) = C(1 - e^{\frac{-3h}{r}}) \quad \dots\dots\dots (5.1)$$

Gaussian Variogram Model

$$\gamma(h) = C(1 - e^{\frac{-3h^2}{r^2}}) \quad \dots\dots\dots (5.2)$$

Spherical Variogram Model

$$\gamma(h) = C[1.5 \frac{h}{r} - 0.5(\frac{h}{r})^3] \quad \dots\dots\dots (5.3)$$

Linear Variogram Model

$$\gamma(h) = C(\frac{3h}{r}) \quad \dots\dots\dots (5.4)$$

Quadratic Variogram Model

$$\gamma(h) = C[\frac{2h}{r} - (\frac{h}{r})^2] \quad \dots\dots\dots (5.5)$$

In practice experimental variogram of the measured data points is estimated and a model variogram which best approximates the shape of the experimental variogram is selected. In (Fig 4.4) model variogram is in red color and experimental variogram in black color that is estimated by measured data points. The model variogram provides a smooth, continuous function for determining appropriate weights for increasingly distant data points.

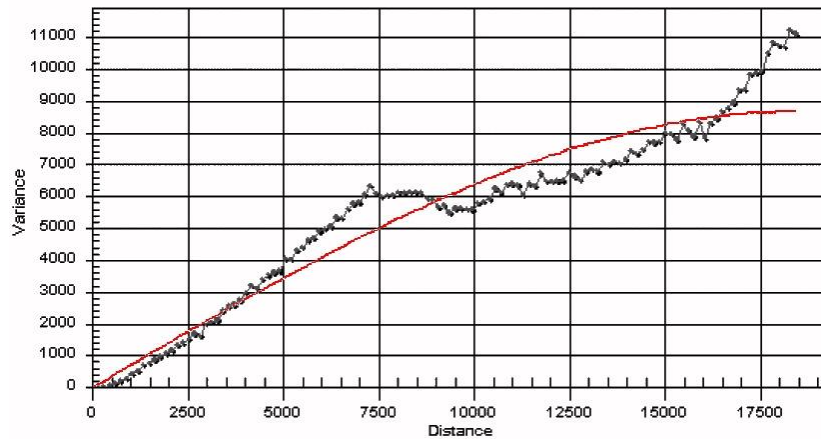


Fig 4.4: Experimental Variogram approximated with Model Variogram

4.3 Trend Surfaces Analysis

Trend surface mapping is a mathematical technique used to compute 2D “plane” or 3D “curves” by using polynomial regression. The grid interpolation techniques can be classified into two classes; global fit and local fit. As the name suggests, global-fit procedures calculate a single function describing a surface that covers the entire map area. The function is evaluated to obtain values at the grid nodes. In contrast, local-fit procedures estimate the surface at successive nodes in the grid using only a selection of the nearest data points. It is most widely used global fitting surface method. It is used to define large scale trends, patterns and provide general structure of spatial variation in large datasets. Local extreme values will affect the trends.

The mapped data are approximated by a polynomial expansion of the geographic coordinates of the control points, and the coefficients of the polynomial function are found by the method of least squares (Tomislav, 2011). It should be insured that the sum of the squared deviations from the trend surface is minimum (Roger, 2005). The polynomial can be expanded to any degree, although there are computational limits because of rounding error. Through the procedure given in Fig. 4.5 moving along the dashed lines, polynomial equations of order 1 to 3 can be constructed.

	0	1	2	3	4
0	1	x	x^2	x^3	x^4
1	y	xy	x^2y	x^3y	
2	y^2	xy^2	x^2y^2	x^3y^2	
3	y^3	xy^3	x^2y^3	x^3y^3	
4	y^4				

Fig 4.5: Procedure to construct trend surface polynomial equations of order 1 to 3.

Order 1: 1*1- simple planar

$$Z = a_0 + a_1x + a_2y \quad \dots\dots\dots (5.6)$$

Order 2: 1*1- Bi-Linear Saddle

$$Z = a_0 + a_1x + a_2y + a_3xy \quad \dots\dots\dots (5.7)$$

Order 2: 2*2- Quadratic

$$Z = a_0 + a_1x + a_2y + a_3x^2 + a_4xy + a_5y^2 \dots\dots\dots (5.8)$$

Order 3: 3*3- Cubic

$$Z = a_0 + a_1x + a_2y + a_3x^2 + a_4xy + a_5y^2 + a_6x^3 + a_7x^2y + a_8xy^2 + a_9y^3 \dots\dots\dots (5.9)$$

Z is dependant variable, **x** and **y** =geographic coordinates (independent variables)

$$a_0, a_1, a_2, \dots a_n = \text{unknown coefficients}$$

The degree of the polynomial will define the number of coefficients. Higher the degree of polynomial, higher will be number of coefficients. By solving simultaneous linear equations, these unknown coefficients are calculated. Three equations are needed to find three unknown coefficients for a first degree polynomial equation. These equations in matrix form will be as:

$$\begin{bmatrix} n & \sum x & \sum y \\ \sum x & \sum x^2 & \sum xy \\ \sum y & \sum xy & \sum y^2 \end{bmatrix} * \begin{bmatrix} a_0 \\ a_1 \\ a_2 \end{bmatrix} = \begin{bmatrix} \sum Z \\ \sum xZ \\ \sum yZ \end{bmatrix} \dots\dots\dots (5.10)$$

Once the coefficients have been estimated, the polynomial function can be evaluated at any point within the map area. It is very simple to create a grid matrix of values by substituting the coordinates of the grid nodes into the polynomial and then for each node calculate an estimate of the surface. Due to least-squares fitting procedure, no other polynomial equation of the same degree can give a better approximation of the data.

The boundaries of a grid are the most imprecise zones, while accuracy of map is centered on the midpoint of the 2D grid. There may be a strong divergence between actual values and computed trend value, away from the midpoint.

4.4 Universal Kriging

Universal Kriging uses the same variogram model as discussed in Ordinary Kriging for spatial interpolation. The main difference is in the selection of data points. Unlike the Ordinary Kriging, where a search criteria is used Ordinary Kriging uses the complete set of XYZ data points similar to Trend Surface. Universal Kriging assumes a general polynomial trend model, such as linear trend model over the whole data range. Thus the resulting trend gives regionalized effect rather than localized effect.

Chapter 5 Geostatistical Mapping

5.1 Introduction

Ordinary Kriging, Trend Surface analysis and Universal Kriging techniques are used to analyze and model the topographic variations of sedimentary cover of Lower Indus Basin. The input data used for this process is formation top of 461 wells. After the initial processing the data is formatted in such a way that it becomes easy to extract the information of just selected formations. Statistical analysis is carried out on the data to estimate variance and standard error between the generalized model surfaces. It was found that some points lie outside the acceptable limits and there is also some redundancy in data points. To remove these errors two filters, Duplication Filter and Standard Deviation Filter, are applied to the data.

Surfaces of different formations are generated by using Ordinary Kriging, Trend surface analysis and Universal Kriging techniques. Ordinary Kriging gives more detail in terms of local variations while Universal Kriging provides the regional trend. Trend surface analysis uses polynomial regression of increasing order to decompose 3D surfaces into sequence of component surfaces. Surfaces of high orders are generated to effectively account the variation in formation tops. But surfaces of high orders cannot be generated due to complex geometry problems.

Initially Universal Kriging was selected as final technique on the bases of standard deviation and standard error value, but after some tests it was found that Ordinary Kriging along with a smoothing operator of very high order produces similar results. To compromise between localized and regional trends Ordinary Kriging along with smoothing kernel operator of 21*21 points. A complete set of statistical analyses are carried out on surfaces of all formations. The processing workflow is given in Fig 5.1.

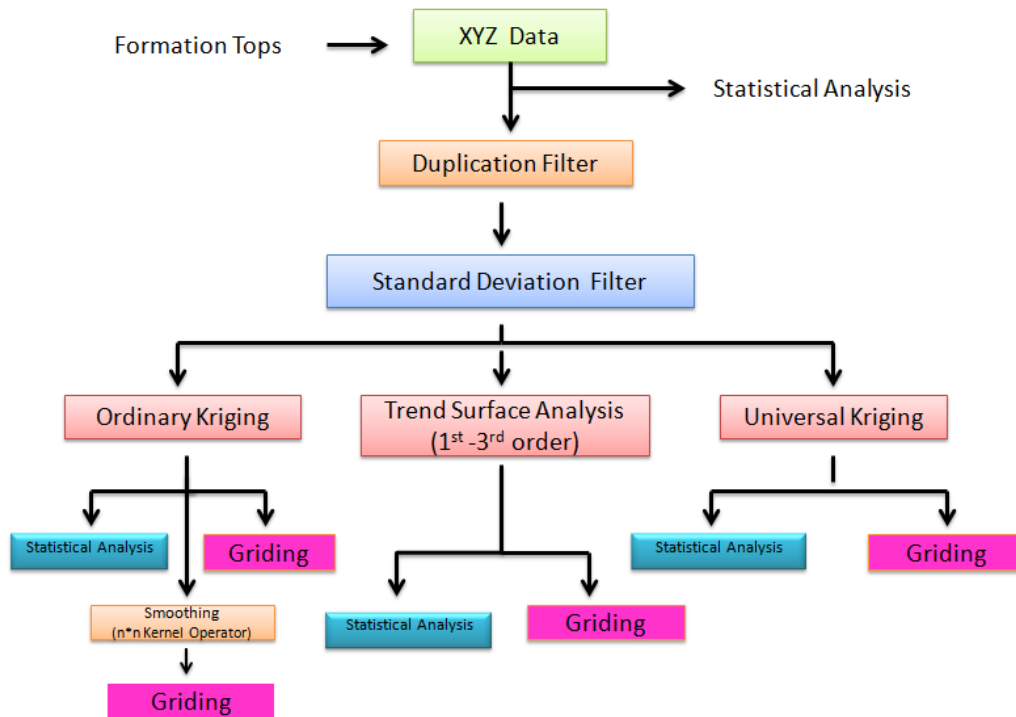


Fig 5.1: Geostatistical Gridding and Analysis Workflow.

The above workflow is implemented in K-tron GridWorks to carryout Geostatistical modeling multiple surfaces in lower Indus basin. This software generates grid files of selected formations using the previously discussed Geostatistical techniques; Ordinary Kriging, Universal Kriging, Smooth Ordinary Kriging and Trend Surface analysis up to a maximum 12th order. The interface of this tool while generating grid files and Geostatistical analysis of Laki is shown in Fig 5.2.

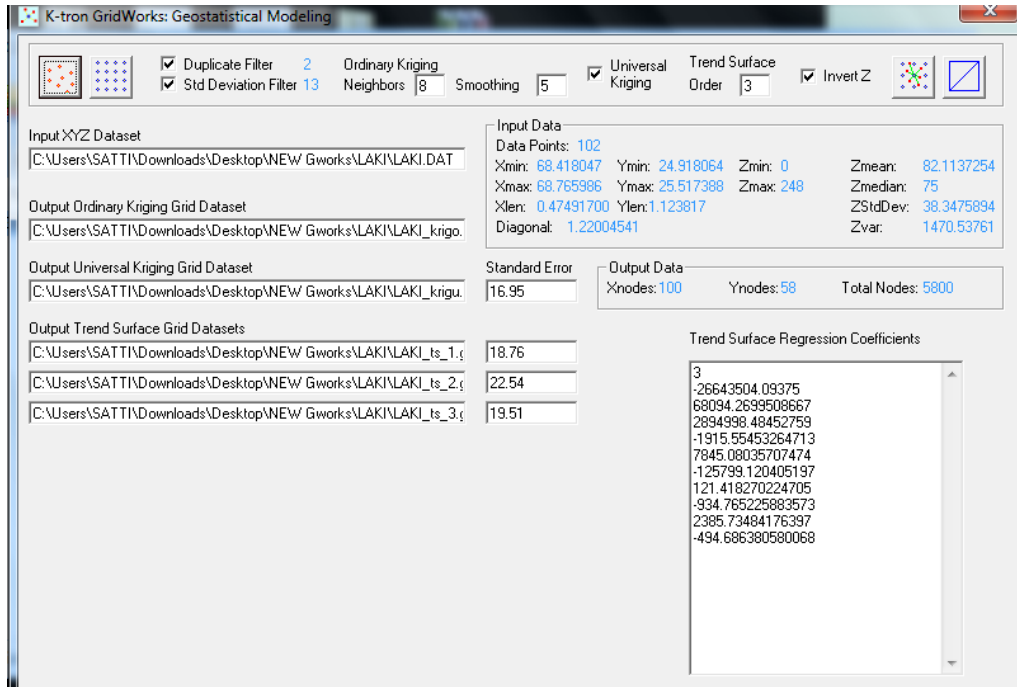


Fig 5.2: User Interface of K-tron GridWorks used for Geostatistical Modeling

5.2 Kirthar Formation

Kirthar is mainly composed of carbonates of Eocene age. General elevation of Kirthar varies from 0 to 508.99 meters. Mean top of Kirthar is 110.5 meters. 3D surfaces of Kirthar are generated using Ordinary Kriging, Trend Surfaces of 1st and 2nd order and Universal Kriging. Ordinary Kriging gives detailed subsurface geometry covering the general gradient along with local highs and lows. The prime objective of this study is to model the regional trend along with prominent geometric variations. Trend Surfaces of 1st and 2nd order are generated which simply provide the regional gradient of formation. In comparison with trend surfaces, Universal Kriging provides a much better surface, but it has been found that Ordinary Kriging along with a smoothed operator of 21 x 21 nodes provides an even better subsurface geometry. Thus smoothed Ordinary Kriging is selected as the final technique for geostatistical modeling of subsurface formations.

5.2.1 Statistical Analysis of Kirthar Formation

Standard error represents the average distance that the observed values fall from the regression line. It measures the accuracy of predictions. Selection of final surface depends on value of standard deviation, and value of standard deviation is obtained from square root of variance. Variance gives information about distribution data points about the mean value.

$$\sigma = \sqrt{\sum \frac{(X - \mu)^2}{N}}$$

Here;

σ = Standard Deviation, μ = Mean of data points

X = Individual data point, N = Number of data points

Statistical analysis of Kirthar Formation is given shown in Table 2. It can be seen that the value of standard deviation decreases by increasing the order of trend surface. In case of Universal Kriging the standard deviation reduces to 30.64.

Table 2: Statistical Analysis of Kirthar Formation

Data	N	Min	Max	Mean	Std Dev	Variance
XYZ	221	0	508.99	129.73	96.45	9302.43
XYZ-Filtered	204	0	245.35	110.47	69.20	4789.15
Ordinary Kriging	3900	0.44	230.42	108.32	54.23	2941.35
Trend Surface 1	3900	-71.85	288.14	108.14	74.80	5595.09
Trend Surface 2	3900	-57.05	274.37	113.72	74.23	5510.22
Universal Kriging	3900	67.43	171.94	110.73	30.64	939.28

5.2.2 Standard Error of Kirthar Formation

Standard error analysis is performed by computing the difference of each surface relative to Ordinary Kriging. Generally the standard error decreases as we move from trend surfaces of higher order. For Kirthar Formation the standard error decreases up to the 2nd order then sharply increased from 33.72 to 54.35 as shown in Table 3. Thus 2nd order trend surface equation is

selected as the best fit surface. The standard error of Universal Kriging surface further reduces to 25.43, providing a geostatistically reliable subsurface model.

Table 3: Standard Error of Kirthar Formation

Grid	Standard Error
Trend Surface (1 st order)	36.6
Trend Surface (2 nd order)	33.72 (selected order)
Trend Surface (3 rd order)	54.35
Universal Kriging	25.43

5.2.3. Histogram Analysis of Kirthar Formation

Histogram is the graphical representation of frequency of distribution of data. In case of Kirthar a total of 221 data points contain the Kirthar formation tops. The histogram of XYZ data (Fig 5.2A) shows a wide data range as some points show large fluctuations as compared to the mean value of 129.73 meters. However, most of the data is clustered around the mean value. After applying the filters 17 large values are removed and the mean value is reduced to 110.5 meters as shown in Fig 5.3B. Histograms of Ordinary and Universal Kriging are also shown in Figs 5.3C and D. It can be seen that most of the values range between 45 to 65 meters.

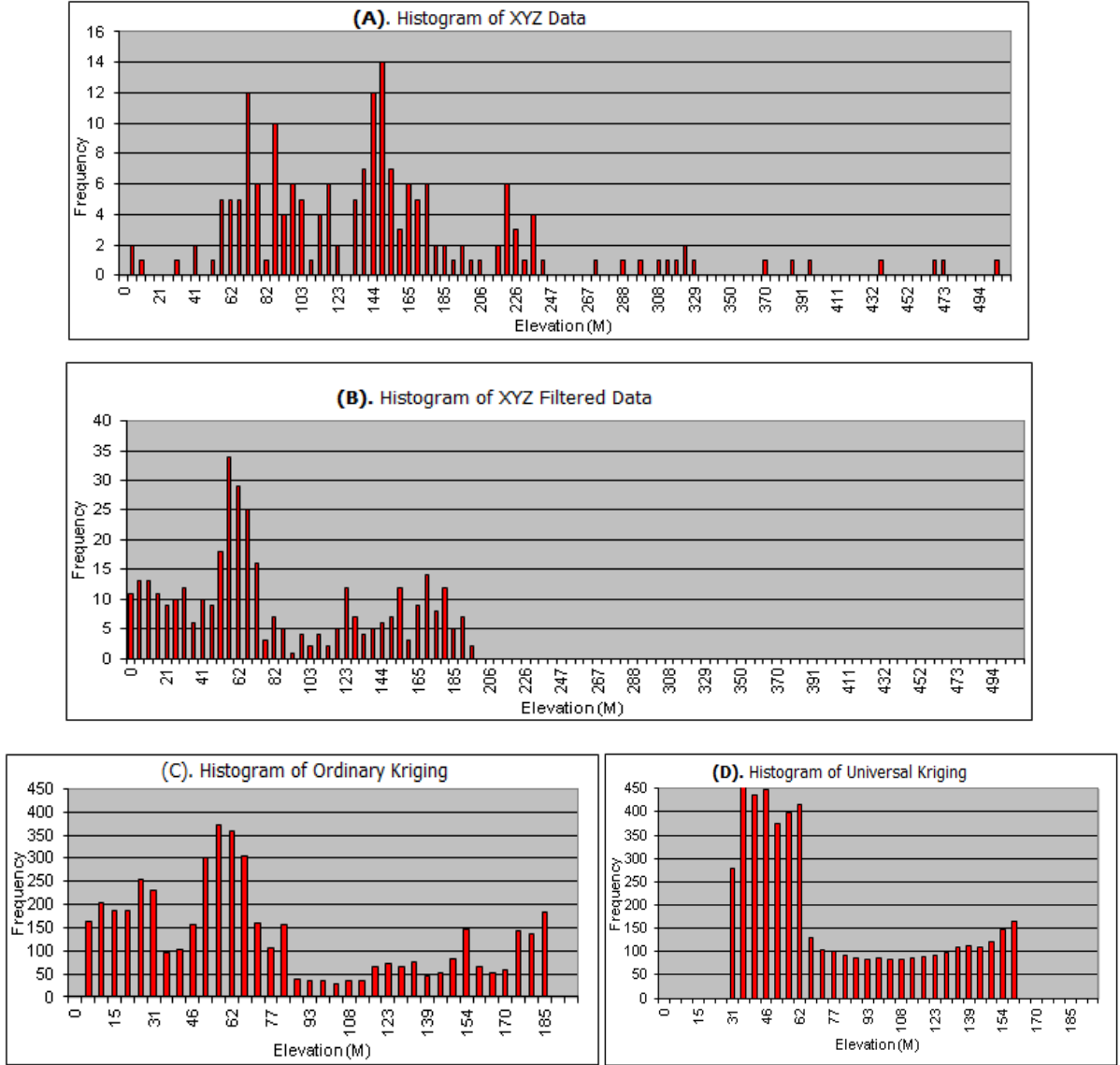


Fig 5.3: Histograms of XYZ data (A), XYZ Filtered data (B), Ordinary Kriging (C) and Universal Kriging (D).

5.2.4. 3D surfaces of Kirthar

3D surfaces of Kirthar formation are generated using Ordinary Kriging, Trend Surface of 1st and 2nd order and Universal Kriging as shown in Fig 5.4. General gradient of the formation is from North to South. Ordinary Kriging shows the local geometric variations where the north western part of the formation is shallow and south western part is getting deeper. Local High and lows can be explained through color bar as shown in Fig 5.4. Ordinary Kriging gives very detail sub surface model, but to model the regional trend with prominent high and lows, trend surfaces of 1st and 2nd order are generated. 1st order trend surface is a flat plane with slope inclined in

direction of mean gradient (N-S) throughout the Lower Indus Basin. As 1st order trend surface equation does not represent a best fit surface therefore higher trend surface equations are required to model the formation tops. 2nd order surface has single flexure along with plane and can be considered to represent the regional trend of Kirthar formation. The 2nd order polynomial has 6 unknown coefficients. To determine these six coefficients, six simultaneous equations are needed. The 2nd Order polynomial equation is;

$$Z_{Kirthar} = -1813828.190 + 63624.081\lambda - 30798.576\phi - 507.619\lambda^2 + 261.149\lambda\phi + 256.341\phi^2 \quad \dots\dots (5.1)$$

Here λ is Longitude and ϕ is Latitude, both are independent variables.

$$a_0 = -1813828.190, a_1 = 63624.081, a_2 = -30798.576,$$

$$a_3 = -507.619, a_4 = 261.149 \text{ And } a_5 = 256.341$$

Universal Kriging surface gives the regional trend of formation by using all data points in computation of variogram. To model the regional trend along with prominent variations, a smoothing Kernel operator of 21*21 points is applied to Ordinary Kriging surfaces.

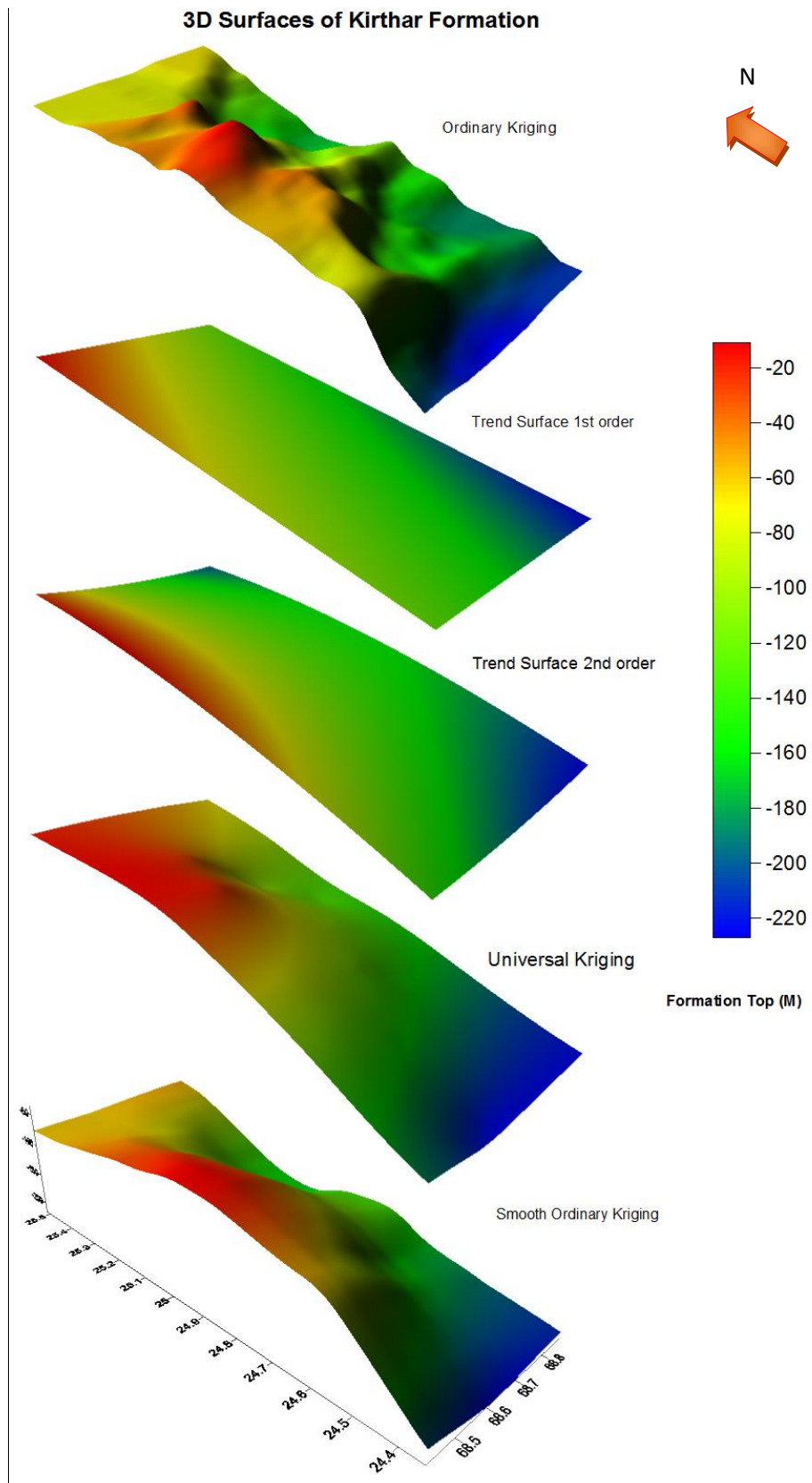


Fig 5.4: 3D Surfaces of Kirthar Formation

5.3 Laki Formation

Laki Formation is mainly composed of carbonates of early Eocene age. General elevation of Laki varies from 0 to 470 meters. Mean top of Laki Formation is 118.6 meters. 3D surfaces of Laki Formation are also generated using Ordinary Kriging, Trend Surfaces of 1st, 2nd and 3rd order and then by Universal Kriging. Ordinary Kriging gives detailed subsurface geometry covering the general gradient along with local highs and lows. The prime objective of this study is to model the regional trend along with prominent geometric variations. Trend Surfaces of 1st, 2nd and 3rd order are generated which provide the regional gradient of formation. Smoothed Ordinary Kriging is selected as the final technique for geostatistical modeling of sub-surface formations. Reason behind this is Ordinary Kriging along with a smoothed operator of 21 x 21 nodes provides an even better subsurface geometry In comparison with Universal Kriging.

5.3.1 Statistical Analysis of Laki Formation

The standard deviation is 111.0777 in XYZ data, but by applying Standard Deviation Filter standard deviation reduced to 38.347. The value of standard deviation is decreases by increasing the order of trend surface and reduced to 32.341 for 3rd order. In case of Universal Kriging standard deviation is 7.494 as shown in Table 4. Statistical analysis of Laki Formation is given shown in Table 4.

Table 4: Statistical Analysis of Laki Formation

Data	N	Min	Max	Mean	Std Dev	Variance
XYZ	117	0	470	118.61	111.07	12338.26
XYZ-Filtered	102	0	248	82.11	38.34	1470.54
Ordinary Kriging	5800	29.97	161.24	79.11	28.63	819.75
Trend Surface 1	5800	17.11	161.18	89.14	37.82	1430.53
Trend Surface 2	5800	11.95	173.72	94.92	35.71	1275.21
Trend Surface 3	5800	6.97	202.98	86.79	32.34	1045.87
Universal Kriging	5800	69.87	101.15	83.31	7.49	56.17

5.3.2 Standard Error of Laki Formation

Standard error of Laki Formation for Trend Surface of 1st order is 18.74, of 2nd order is 22.54 and again it reduced to 19.54 for 3rd order. Thus 3rd order grid is selected. Standard error is 16.95 in case of Universal Kriging, which is small value in comparison with Trend Surface (increasing orders) shown in Table 5.

Table 5: Standard Error of Laki Formation

Grid	Standard Error
Trend Surface (1 st order)	18.74
Trend Surface (2 nd order)	22.54
Trend Surface (3 rd order)	19.54 (<i>selected order</i>)
Universal Kriging	16.95

5.3.3 Histograms Analysis of Laki Formation

In case of Laki Formation 117 meters total data points were found in XYZ data having mean value 118.6 meters and Fig 5.5A shows large fluctuations as compared to the mean value of 118.6 meters. Data points which are producing large fluctuations are removed and the mean value reduced to 82. Histograms of XYZ and XYZ Filtered data are shown in Fig 5.5A and Fig 5.5B.

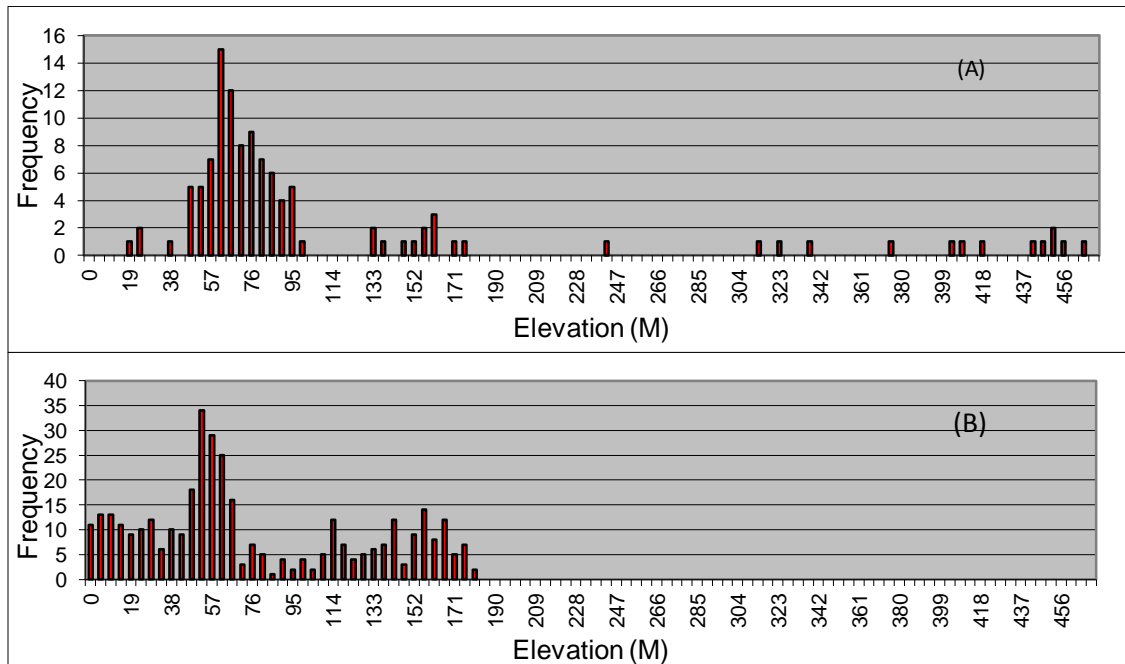


Fig 5.5: Histograms of Laki Formation of XYZ (A) and XYZ filtered data (B)

5.3.3 3D surfaces of Laki Formation

3D surfaces of Laki are generated using Ordinary Kriging, Trend Surface of 3rd order and then by Universal Kriging as shown in Fig 5.6. General gradient of the formation is from north to south. Ordinary Kriging gives the local geometric variations along with general gradient. Surface shows that North eastern part of formation is at greater depths and South Western and North eastern part is comparatively shallow. Trend Surfaces of 1st and 2nd order do not passes as best fit through the data points due to complexity of best fit surface and because of variations. Thus 3rd order trend surface passes as best fit, the equation derived for this have maximum power 3 with ten unknown coefficients. 3rd order surface have double flexure along with plane and shows the regional gradient of Laki Formation that is NS. Equation is the 3rd Order polynomial equation.

$$\begin{aligned} Z_{Laki} = & -26643504.093 + 68094.269 \lambda + 2894998.484 \phi - 1915.554 \lambda^2 + 7845.080 \lambda \phi \\ & - 125799.120 \phi^2 + 121.418 \lambda^3 - 934.765 \lambda^2 \phi + 2385.734 \lambda \phi^2 \\ & - 494.686 \phi^3 \quad \dots \dots \dots (5.2) \end{aligned}$$

Like the previous Surfaces Universal Kriging gives the regional trend of formation thus to analyze the regional trend along prominent local high and lows, a smoother of 21x21 points is applied on Ordinary Kriging. Here only selected surfaces i.e. Ordinary Kriging, Trend Surface 3rd order, Universal Kriging and Smooth Ordinary Kriging are shown in the Fig 5.6.

3D Surfaces of Laki Formation

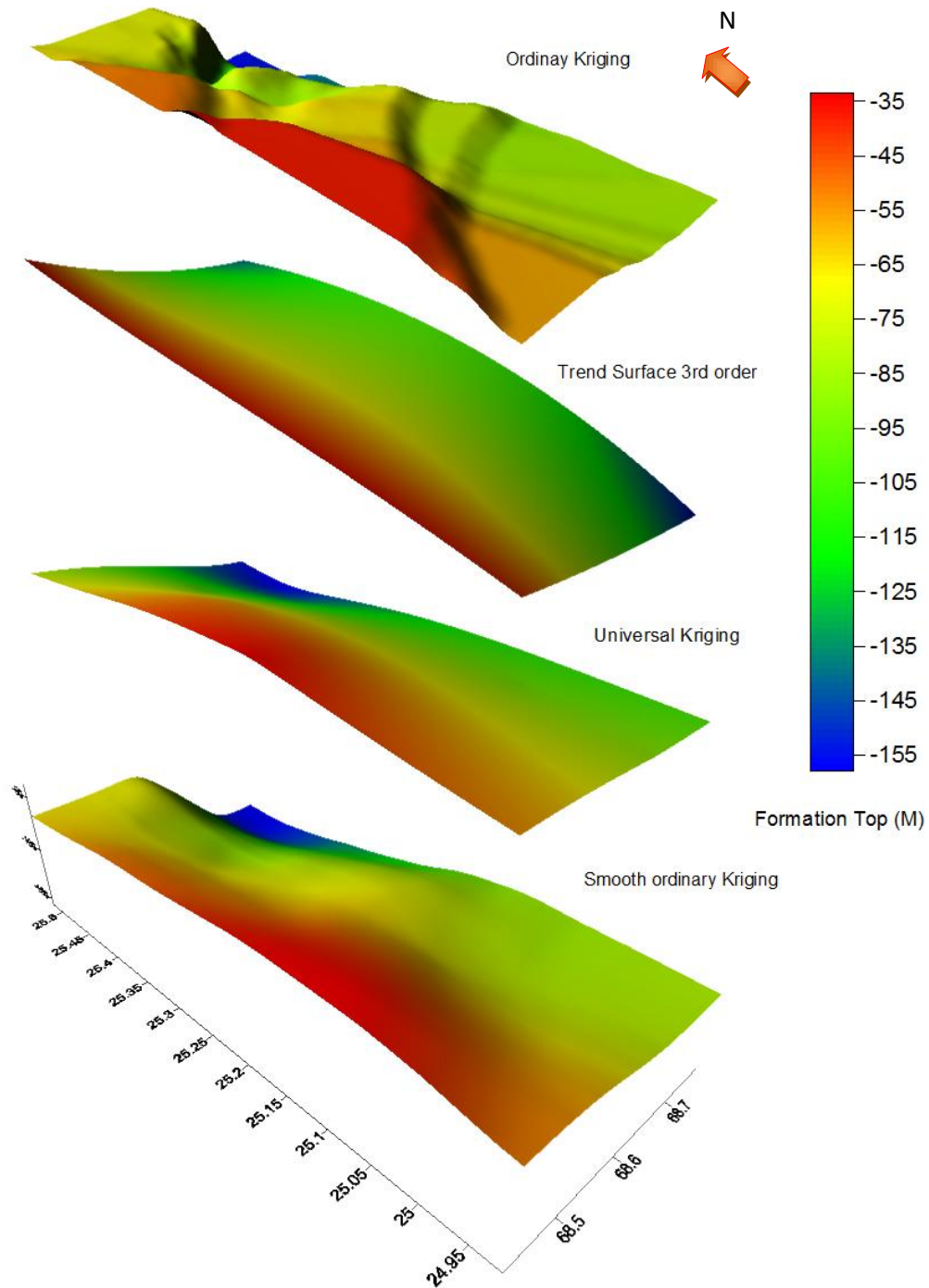


Fig 5.6: 3D Surfaces of Laki Formation

5.4 Ranikot Group

Ranikot of Paleocene age is subdivided into two parts, Upper and Lower Ranikot. The upper part consists of Lakhra Formation and the lower part consists of Khadro Formation followed by Bara Formation.

5.4.1 Upper Ranikot Formation

Upper Ranikot is of Paleocene age, consists of Lakhra Formation. It is mainly composed of Limestone with sandstone and shale. General elevation of Upper Ranikot is varying from 0 to 934 meters. Mean top of Upper Ranikot Formation is 154 meters. Like Laki, 3D surfaces of Upper Ranikot are also generated using Ordinary Kriging, Trend Surfaces of 1st, 2nd and 3rd order and then by Universal Kriging. On the bases of standard error value 3rd order of Trend surface is selected to analyze the regional trend. General gradient of Upper Ranikot is from north to south.

5.4.1.1 Statistical Analysis of Upper Ranikot Formation

The standard deviation for 3rd order of Trend Surface is 73.540, which is less than 2nd order as shown in Table 6. In case of Universal Kriging standard deviation reduced to 7.494. Thus Universal Kriging surface will give the regional trend of formation top of Laki. Statistical analysis of Laki Formation is given shown in Table 6.

Table 6: Statistical Analysis of Upper Ranikot

Data	N	Min	Max	Mean	Std Dev	Variance
XYZ	370	0	934	153.94	179.22	32120.67
XYZ-Filtered	345	0	410	121.12	126.23	15934
Ordinary Kriging	5200	1.61	363.48	126.13	84.12	7076.28
Trend Surface 1	5200	-17.2	317.21	150.00	69.80	4872.5
Trend Surface 2	5200	-111.26	282.98	115.44	77.46	6000.01
Trend Surface 3	5200	-162.67	362.02	103.45	73.54	5408.13
Universal Kriging	5200	40.35	234.25	132.11	48.43	2345.8

5.4.1.2 Standard Error of Upper Ranikot Formation

Standard error of Upper Ranikot for Trend Surface of 1st is 54.71, of 2nd order is 56.15 and again it reduced to 38.75 for 3rd order. Thus 3rd order grid is selected. Standard error is 34.27 in case of Universal Kriging, which is less than Trend Surface (increasing orders) shown in Table 8.

Table 8: Standard Error of Upper Ranikot

Grid	Standard Error
Trend Surface (1 st order)	54.71
Trend Surface (2 nd order)	56.15
Trend Surface (3 rd order)	38.75(selected order)
Universal Kriging	34.27

5.4.1.3. Histogram Analysis of Upper Ranikot

Histogram is the graphical representation of frequency of distribution of data. In case of Upper Ranikot a total of 370 data points contain the Upper Ranikot tops. The histogram of XYZ data (Fig 5.7A) shows a wide data range as some points show large fluctuations as compared to the mean value of 153.9 meters. However, most of the data is clustered around the mean value. After applying the filters large values are removed and the mean value is reduced to 121.12 meters as shown in Fig 5.7B.

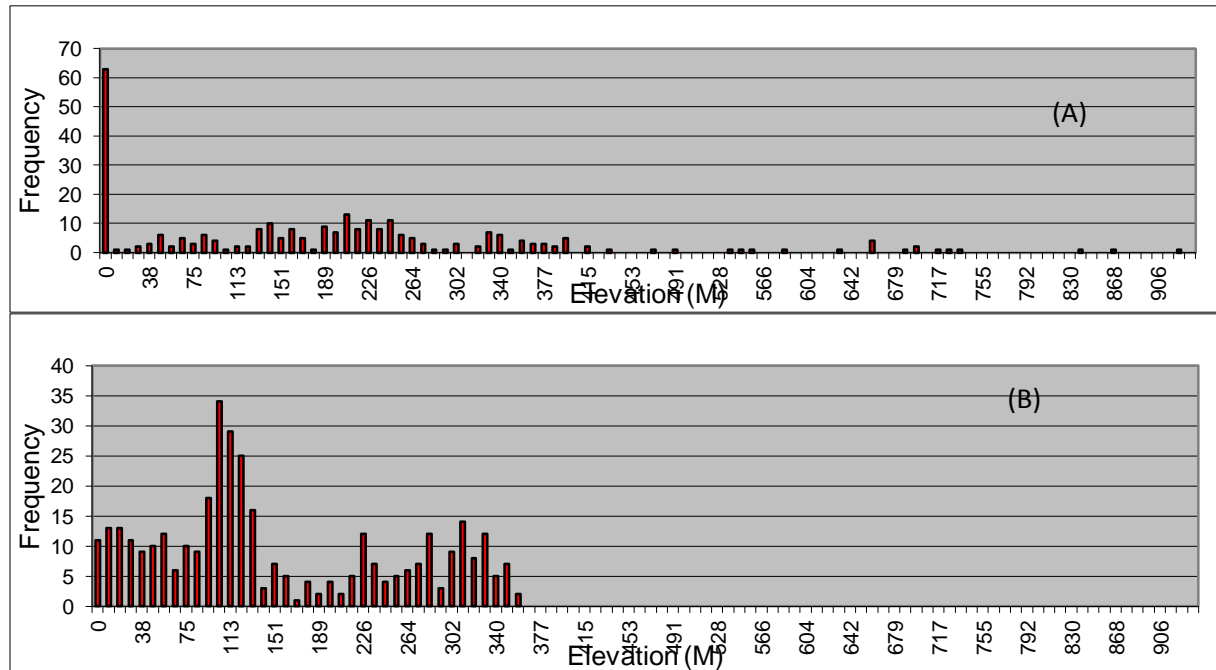


Fig 5.7: Histograms of XYZ (A) and XYZ filtered data (B) of Upper Ranikot

5.4.1.3 3D Surfaces of Upper Ranikot

3D surfaces of Upper Ranikot are generated in the similar ways as the previous formations. Ordinary Kriging show the local variations, formation is at greater depths up to 340 meters at southern part and is comparatively shallow towards North. Local High and lows can be explained through color bar as shown in Fig 5.8. 3rd order trend surface passes as best fit, thus the equation is also derived for this. 3rd order surface have double flexure and shows the regional gradient of Upper Ranikot that is NS. Equation of 3rd Order polynomial is;

$$\begin{aligned} Z_{U_{Ranikot}} = & 94475229.775 - 2494435.254 \lambda - 4648432.727 \phi + 47063.801 \lambda^2 - \\ & 54550.382 \lambda \phi + 261220.498 \phi^2 - 379.623 \lambda^3 + 1213.555 \lambda^2 \phi - 2242.223 \lambda \phi^2 - \\ & 1434.93 \phi^3 \quad \dots \dots \dots (5.3) \end{aligned}$$

Like the previous Surfaces Universal Kriging gives the regional trend of formation. For regional trend with local prominent variations smoothing of 21x21 points is applied on Ordinary Kriging to get required surface that is smooth Ordinary Kriging surface as shown in Fig 5.8.

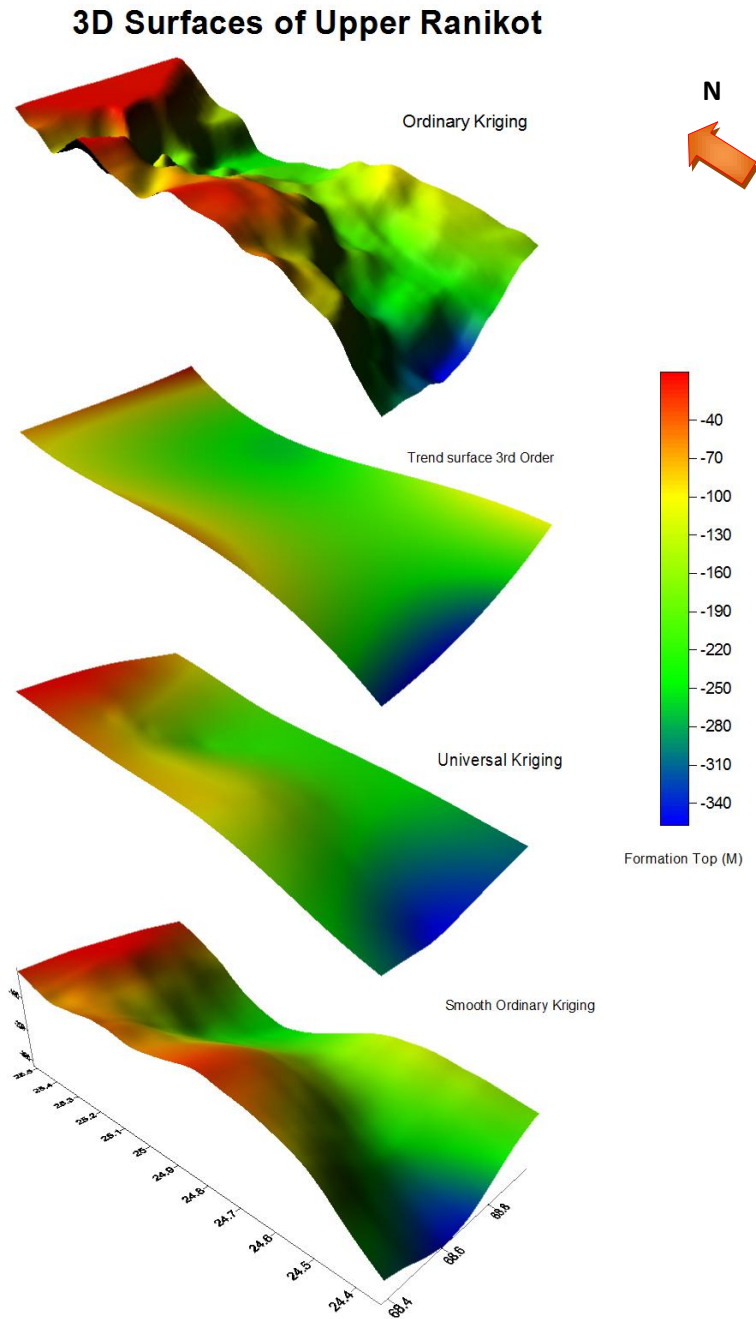


Fig 5.8: 3D surfaces of Upper Ranikot

5.4.2 Lower Ranikot Formation

Lower Ranikot is of Paleocene age; consist of Khadro followed by Bara Formation. Khadro is mainly composed of Limestone and Bara is composed of sandstone and shale. General elevation of is varying from 67.97 to 876.26 meters. Mean top of Lower Ranikot is 317.79 meters.

5.4.2.1 Statistical Analysis of Lower Ranikot Formation

Standard deviation is 139.94 in XYZ data, but by applying Standard Deviation Filter value decreased to 98.20. Standard deviations are 118.17 of 2nd order Trend surface, 52.35 of 1st order and 38.24 is of Universal Kriging as shown in Table 8. Universal Kriging surface will give the regional trend of formation top. Statistical analysis of Lower Ranikot is given shown in Table 9.

Table 9: Statistical Analysis of Lower Ranikot

Data	N	Min	Max	Mean	Std Dev	Variance
XYZ	246	67.97	876.26	336.58	139.93	19582.9
XYZ-Filtered	228	130.45	524.23	317.68	98.20	9643.9
Ordinary Kriging	4500	155.0	467.16	319.17	92.08	8479.7
Trend Surface 1	4500	219.27	419.82	319.55	52.34	2740.30
Trend Surface 2	4500	142.07	705.25	336.87	118.17	13964.8
Universal Kriging	4500	248.26	384.22	316.27	38.24	1462.71

5.4.2. 2 Standard Error of Lower Ranikot Formation

Trend Surface for 2nd order is selected having Standard error of 35.75, which is less than 1st order. Standard error is reduced to 31.67 in case of Universal Kriging as shown in Table 10.

Table 10: Standard Error of Lower Ranikot

Grid	Standard Error
Trend Surface (1 st order)	70.57
Trend Surface (2 nd order)	35.75 (<i>selected order</i>)
Trend Surface (3 rd order)	259.66
Universal Kriging	31.67

5.4.2.3 Histogram Analysis of Lower Ranikot

For Lower Ranikot 246 total data points found in XYZ data and mean value is 336.6 meters. Here variation in data is very large and few values are very large, which are producing large fluctuations from mean value that is 336.6. Most of the data is clustered near the mean value as shown in Fig 5.9A. After applying the filters large values are filtered out, as these are affecting the mean value as shown in Fig 5.9(B). After the filtering the mean value reduced to 317.68.

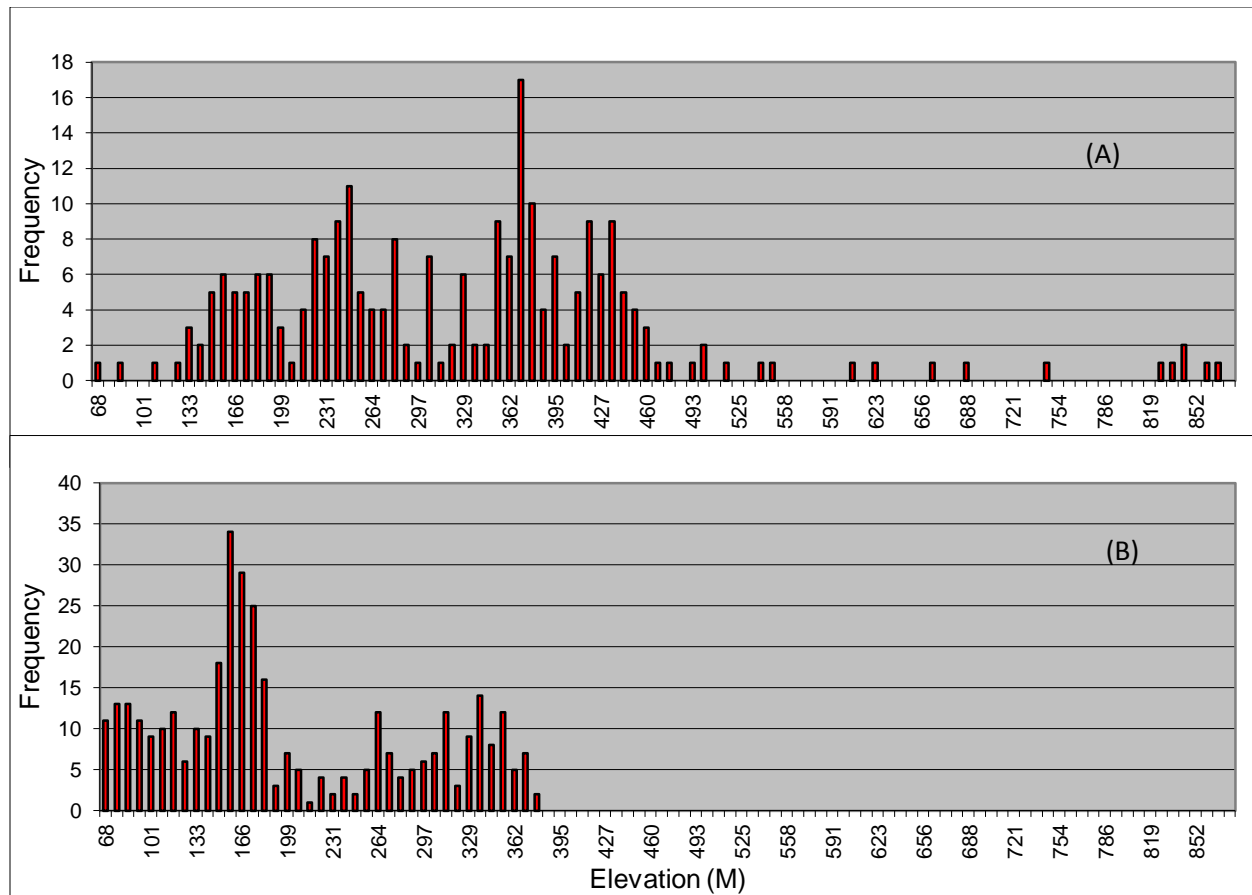


Fig 5.9: Histogram of XYZ (A) and filtered XYZ data (B) of Lower Ranikot

5.4.2.3 3D Surfaces of Lower Ranikot

3D surfaces of Lower Ranikot are generated in the similar ways as the previous formations. Ordinary Kriging show the local geometric variations with local highs and lows. 2nd order trend surface passes as best fit, thus the equation is also derived for it. 2nd order surface shows some shallow structure along East west as shown in Fig 5.10. 2nd Order polynomial equation is;

$$Z_{L_Ranikot} = 4696584.824 - 114530.433 \lambda - 63265.742 \phi + 851.26 \lambda^2 - 71.947 \lambda \phi + 1375.198 \phi^2 \dots\dots\dots (5.4)$$

Like the previous Surfaces Universal Kriging gives the regional trend of formation. To model the regional trend and prominent geometric variations smoothing Kernel operator of 21x21 points is applied on Ordinary Kriging surfaces to get a surface (Ordinary Kriging surface) having regional trend with local variations as shown in Fig 5.10.

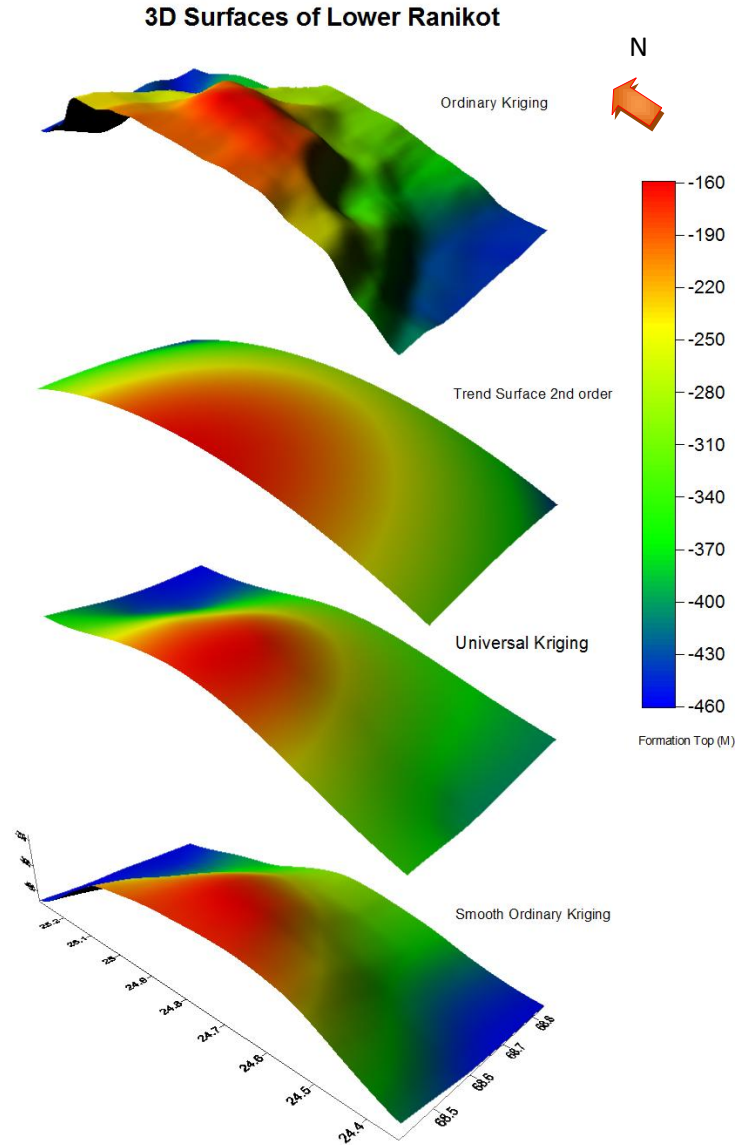


Fig 5.10: 3D Surfaces of Lower Ranikot

5.5 Parh Limestone

Parh Limestone of upper Cretaceous age is mainly composed of Limestone. General elevation of Parh Limestone varies from 427.92 to 1206.34 meters. Mean top of Parh Limestone is 746.67 meters. 3D surfaces of Parh are generated by Ordinary Kriging, Trend Surface 1st and 2nd order and then by Universal Kriging. Ordinary Kriging gives the general gradient and encounters all local highs and lows. The prime objective of this study is to model the regional trend along with prominent geometric variations. So Trend Surface 1st and 2nd order and Universal Kriging are

applied, but this analysis gives regional gradient of formation. Thus to generate regional trend along geometric variations Kernel Operator of 21x21 points applied on Ordinary Kriging. The resulting Smooth Ordinary Kriging surface represents the regional trend and prominent local geometric variations.

5.5.1 Statistical Analysis of Parh Limestone

Standard deviation of Ordinary Kriging, Trend Surface (increasing order) and Universal Kriging is given in Table 11. In Trend Surface analysis 2nd order is selected with standard deviation 152.15. In case of Universal Kriging, standard deviation is 97.4, so it will provide a geostatistically reliable subsurface model.

Table 11: Statistical Analysis of Parh Limestone

Data	N	Min	Max	Mean	Std Dev	Variance
XYZ	311	427.92	1206.34	746.68	214.87	46167.7
XYZ-Filtered	273	427.92	1067	693.95	171.90	29549.9
Ordinary Kriging	4000	444.67	1054.6	655.38	146.27	21396.1
Trend Surface 1	4000	356.21	937.95	647.086	127.96	16374.7
Trend Surface 2	4000	488.06	1219.1	662.53	152.15	23149.5
Universal Kriging	4000	549.27	899.83	657.49	97.5	9496.2

5.5.2 Standard Error of Parh Limestone

2nd order of Trend Surface is selected having Standard error of 34.21, which is less than 1st order. The standard error of Universal Kriging surface further reduces to 29.56, providing a geostatistically reliable subsurface model. Standard error is shown in Table 12.

Table 12: Standard Error of Parh Limestone

Grid	Standard Error
Trend Surface (1 st order)	107.5
Trend Surface (2 nd order)	34.21 (<i>selected order</i>)
Trend Surface (3 rd order)	93.23
Universal Kriging	29.56

5.5.3 Histograms Analysis of Parh Limestone

Histogram is the graphical representation of frequency of distribution of data. 311 data points in XYZ data contain the Parh formation tops with means value is 746.67 meters. Fig 5.11(A) shows wide data range and high values are producing large fluctuations. After the filtering the mean value reduced to 693.94 as shown in Fig 5.11(B). Here most of the data is clustered near the mean value.

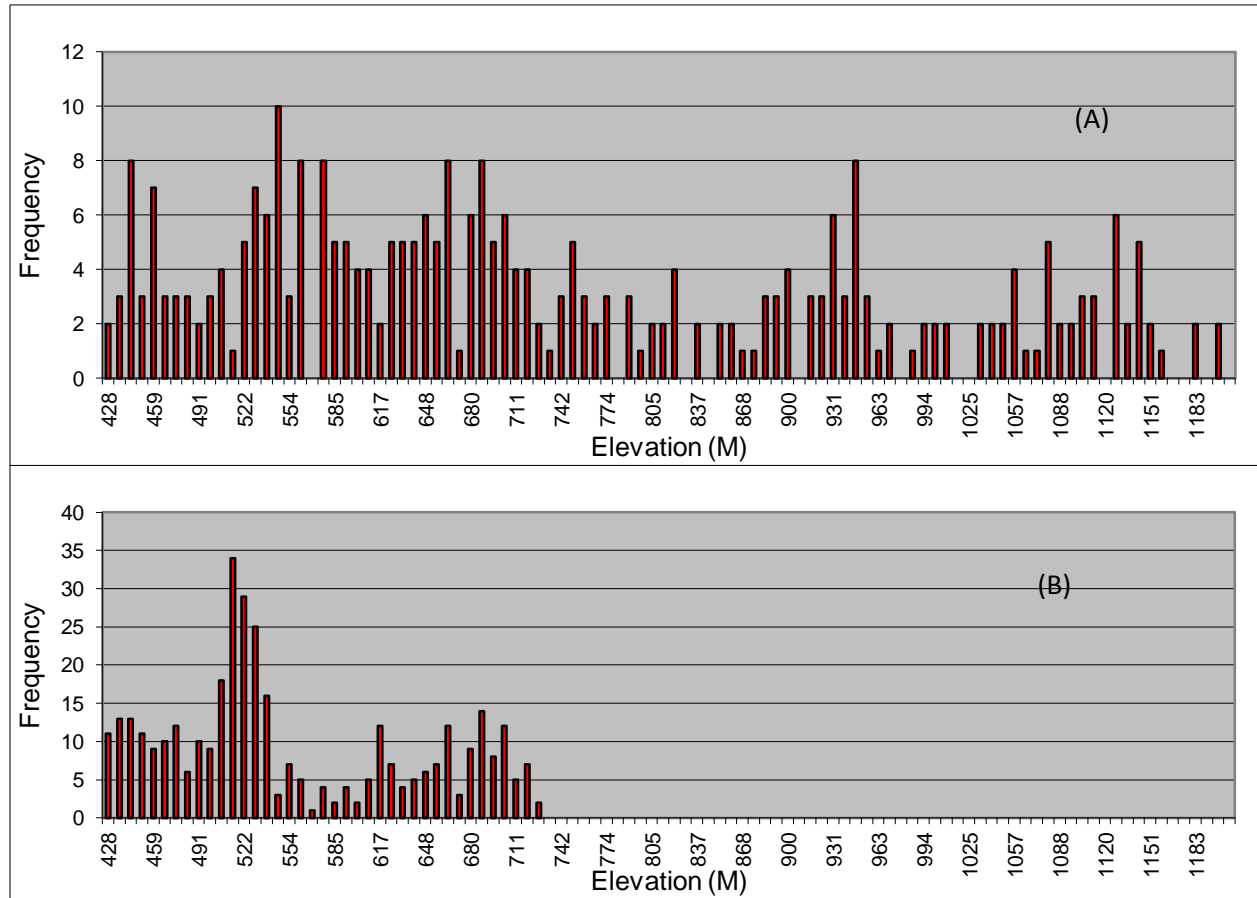


Fig 5.11: Histogram of XYZ (A) and filtered XYZ data (B) of Parh

5.5.3 3D Surfaces of Parh Limestone

3D surfaces of Parh Limestone are generated in the similar way as the previous formations. Ordinary Kriging show the local geometric variations. 2nd order trend surface passes as best fit, thus the equation is also derived for it. 2nd order surface shows some shallow structure along East west and depth increases on other two sides as shown in Fig 5.12. The 2nd Order polynomial equation is;

$$Z_{Parh} = 8809812.52 - 246846.693\lambda - 27610.325\phi + 1914.57\lambda^2 - 640.25\lambda\phi + 1444.55\phi^2 \dots\dots\dots (5.5)$$

Like the previous Surfaces Universal Kriging gives the regional trend of formation showing strong N-S gradient. To model the regional trend and prominent geometric variations smoothing Kernel operator of 21*21 points is applied on Ordinary Kriging surfaces to get a smooth Ordinary Kriging surface. Thus this surface is the model representation of Parh with strong NS gradient.

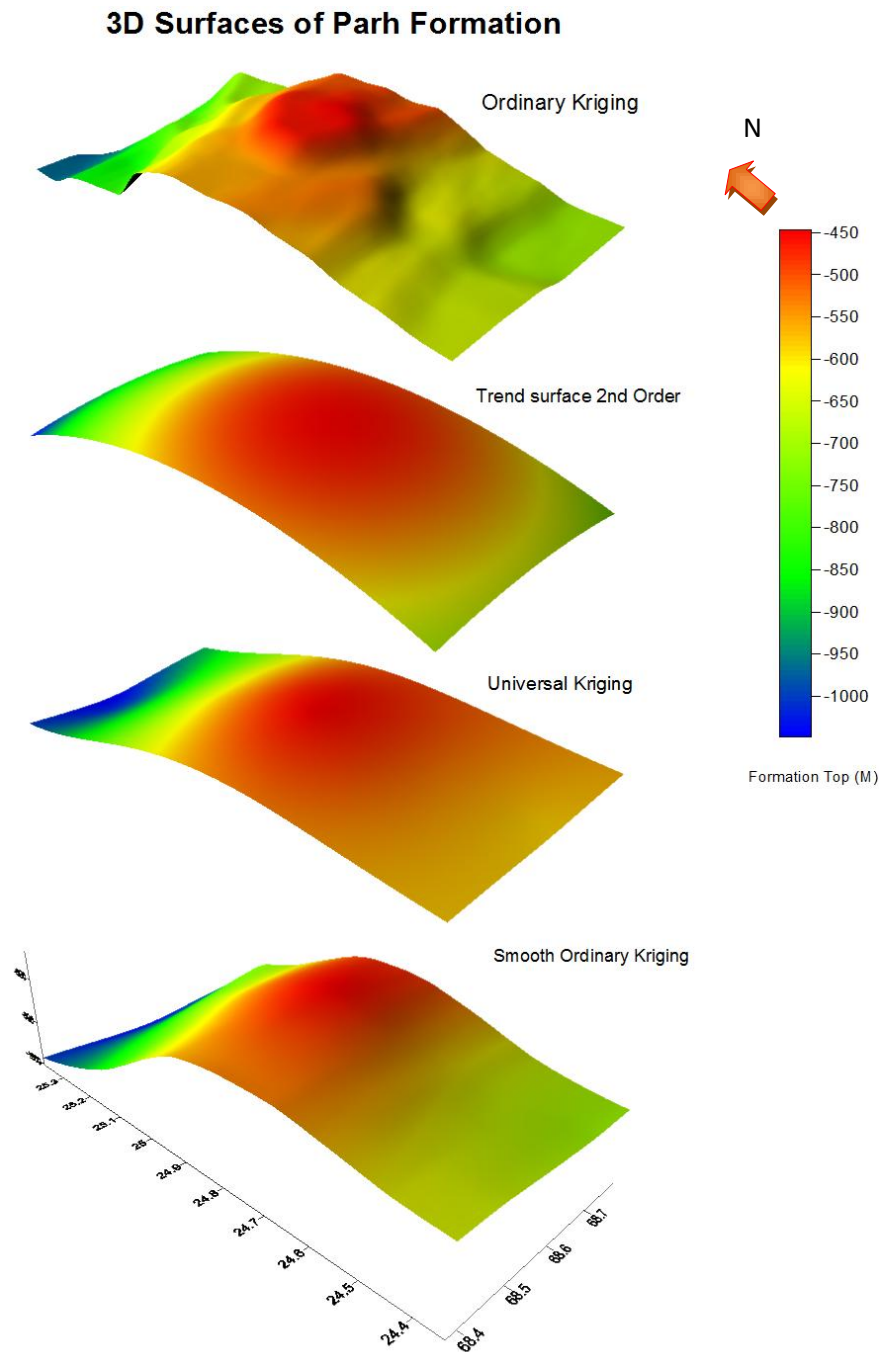


Fig: 5.12: 3D Surfaces of Parh Limestone

5.6 Goru Formation

Goru Formation of Middle Cretaceous age is divided into two units Upper and Lower Goru. Goru Formation is a complete petroleum play. Sands of Lower Goru are producing oil and shales of upper Goru are acting as a seal.

5.6.1 Upper Goru

The Upper Goru is composed of shale or clay and marl and has no reservoir potential, but it forms a thick protective cover for oil and gas reservoirs of Lower Goru. General elevation of Kirthar varies from 496.37 to 2347 meters. Mean top of Upper Goru is 824.98 meters. The prime objective of this study is to model the regional trend along with prominent geometric variations. 3D surfaces of Upper Goru are generated using Ordinary Kriging, Trend Surfaces of 1st, 2nd order and then by Universal Kriging. Ordinary Kriging gives the general gradient and encounters all local highs and lows. Trend Surface of 1st, 2nd order and Universal Kriging are applied, but this analysis gives regional gradient of formation. Thus to analyze regional trend along prominent geometric variations Kernel Operator of 21*21 points is applied on Ordinary Kriging.

5.6.1.1 Statistical Analysis of Upper Goru

Selection of final surface depends on value of standard deviation. Generally the standard deviation decreases as we move from trend surfaces of higher order. In Trend Surface analysis 2nd order is selected with standard deviation 201.550 which is less than 1st order. In case of Universal Kriging standard deviation is 147.83. Standard deviation for Ordinary Kriging, Trend Surface (increasing order) and Universal Kriging is given in Table 13.

Table 13: Statistical Analysis of Upper Goru

Data	N	Min	Max	Mean	Std Dev	Variance
XYZ	398	469.37	2347	824.98	253.74	64383.62
XYZ-Filtered	374	469.37	1204	791.91	208.96	43664.67
Ordinary Kriging	4800	493.24	1182.2	770.66	199.19	39679.05
Trend Surface 1	4800	244.59	1206.1	725.37	204.13	41670.08
Trend Surface 2	4800	501.42	1620.5	773.75	201.5	40622.41
Universal Kriging	4800	596.81	1085.51	766.69	147.82	21852.39

5.6.1.2 Standard Error of Upper Goru

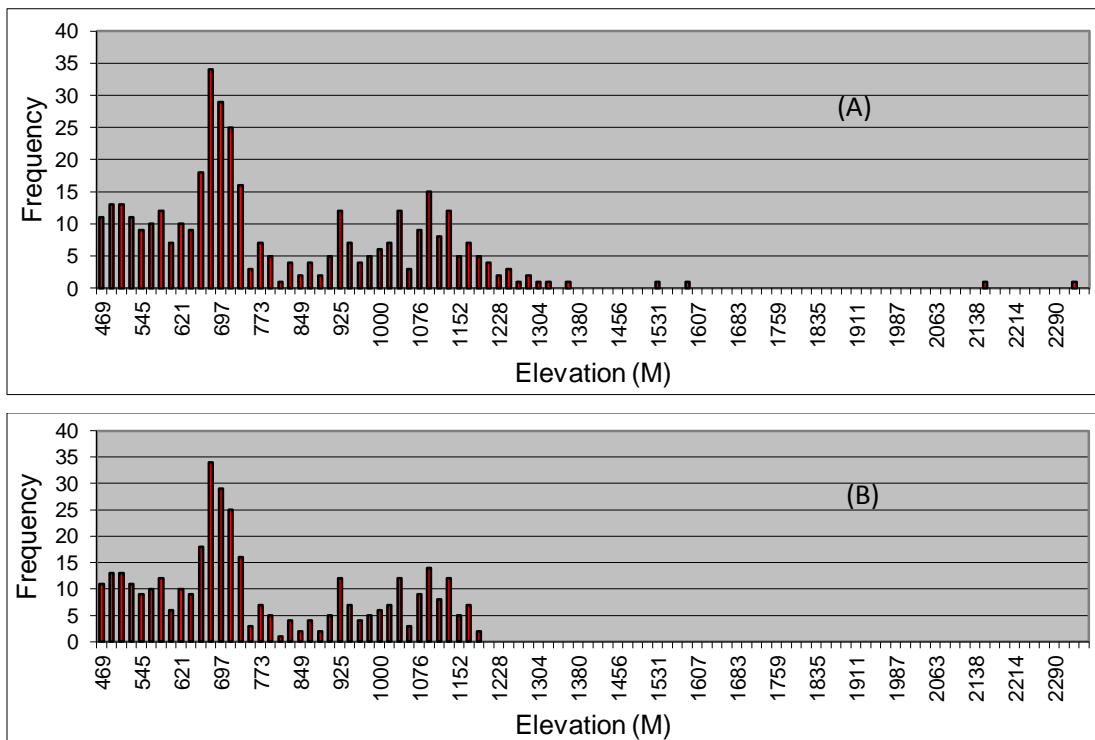
Standard error of Upper Goru Formation for Trend Surfaces of 1st and 2nd order is decreases by increasing order, but at 3rd order value increased from 53.43 to 54.43. Thus 2nd order grid is selected. Standard error reduced to 51.01 in case of Universal Kriging as shown in Table 14.

Table 14: Standard Error of Upper Goru

Grid	Standard Error
Trend Surface (1 st order)	129.46
Trend Surface (2 nd order)	53.43 (<i>selected order</i>)
Trend Surface (3 rd order)	54.23
Universal Kriging	51.01

5.6.1.3 Histogram Analysis of Upper Goru

In case of Upper Goru 398 data points contain the Upper Goru tops. The histogram of XYZ data (Fig 5.13A) shows a wide data range as some points show large fluctuations as compared to the mean value of 824.73meters. However, most of the data is clustered around the mean value. After applying the filters 24 large values are removed and the mean value is reduced to 791.91 meters as shown in Fig 5.13B.

**Fig 5.13:** Histogram of XYZ and XYZ filtered data of Upper Goru

5.6.1.4 3D Surfaces of Upper Goru

3D surfaces of Upper Goru are generated in the similar way as the previous formations. Ordinary Kriging show the local variations i.e. local highs and lows. 2nd order of Trend Surface passes as best fit, thus the polynomial equation is also derived for it. 2nd order of Trend Surface shows

some shallow structure along East west as shown in Fig 5.14. Like the previous Surfaces Universal Kriging gives the regional trend of formation. Smoothing Kernel operator of 21*21 points is applied on Ordinary Kriging surfaces to get a surface having regional trend with local prominent geometric variations. Thus smooth Ordinary Kriging surface is the model representation Of Upper Gore Formation. 2nd Order polynomial equation is;

$$Z_{U_Goru} = 4627988.11 - 121889.815 \lambda - 34633.34\phi + 980.83\lambda^2 - 534.05\lambda\phi + 1440.51\phi^2 \dots \dots \dots (5.6)$$

3D Surfaces of Upper Goru

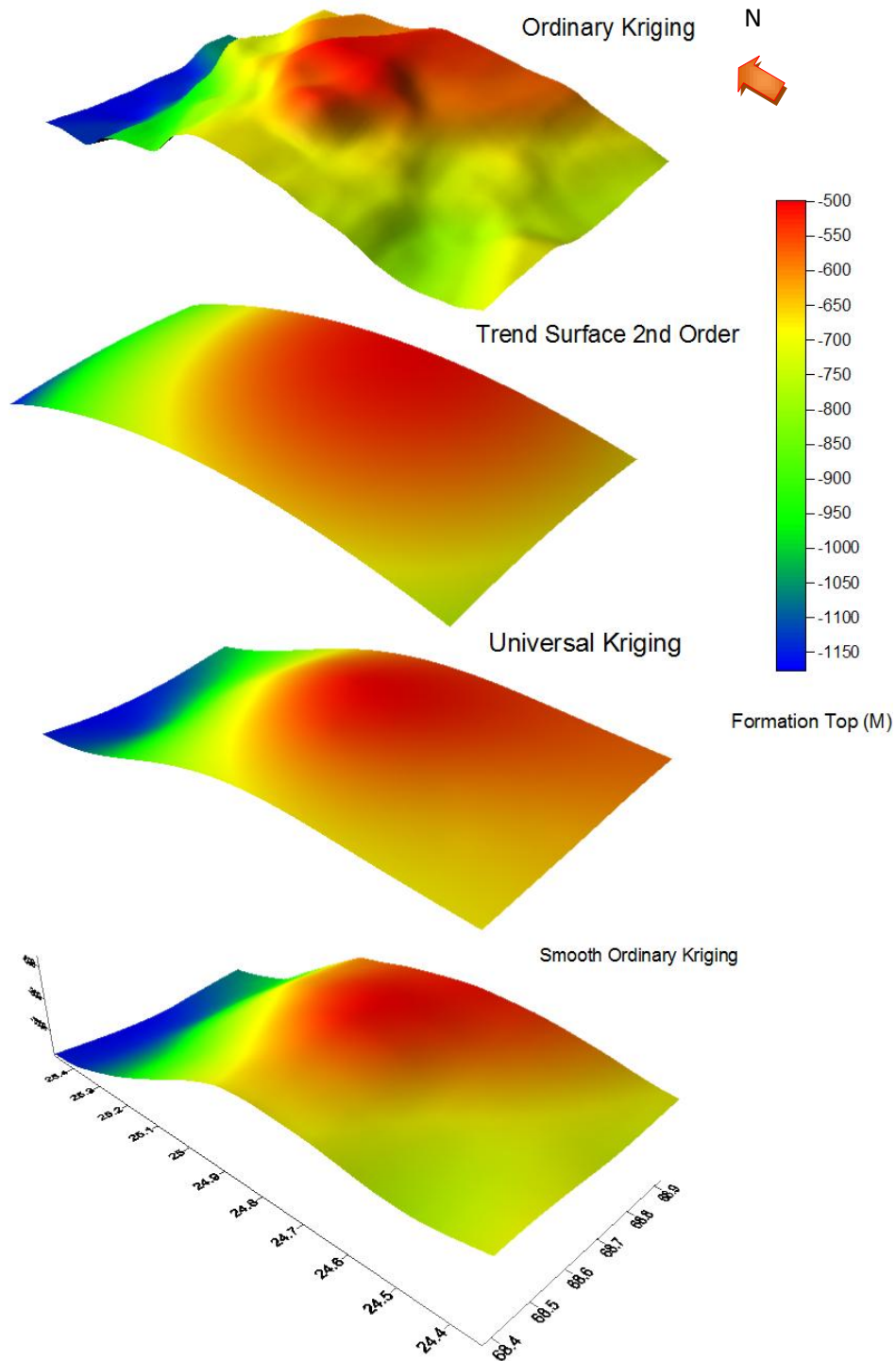


Fig 5.14: 3D surfaces of Upper Goru

5.6.2 Lower Goru Formation

The Lower Goru is mostly composed of interbedded sandstone and shale in different proportions. General elevation of Lower Goru varies from 537.03 to 2598 meters. Mean top of Lower Goru is 1719.43 meters. To generate regional trend along prominent geometric variations, smoothing Kernel Operator of 21*21 points is applied on Ordinary Kriging. The resulting Smooth Ordinary Kriging Surface represents the regional trend and geometric variations of Lower Goru Formation throughout the basin.

5.6.2.1 Statistical Analysis of Lower Goru

In Trend Surface analysis the 2nd order surface is selected to analyze the regional trend with standard deviation 448.002. In case of Universal Kriging standard deviation is 200.12. Standard deviation for Ordinary Kriging, Trend Surface (increasing order) and Universal Kriging is given in Table 15.

Table 15: Statistical Analysis of Lower Goru

Data	N	Min	Max	Mean	Std Dev	Variance
XYZ	396	537.03	2598	1633.56	499.89	249889.2
XYZ-Filtered	340	884.49	2362	1719.43	397.40	157932.7
Ordinary Kriging	4100	1020.41	2289.95	1575.82	348.01	121114.6
Trend Surface 1	4100	421.06	2579.35	1500.21	481.78	232115.1
Trend Surface 2	4100	417.61	2820.2	1480.92	448.00	200705.8
Universal Kriging	4100	1338.47	2070.72	1621.54	200.12	40047.01

5.6.2.2 Standard Error of Lower Goru

2nd order of Trend Surface is selected having Standard error of 208.01, which is less than 1st and 3rd order. Standard error reduced to 157.09 in case of Universal Kriging, as shown in Table 16.

Table 16: Standard Error of Lower Goru

Grid	Standard Error
Trend Surface (1 st order)	211.66
Trend Surface (2 nd order)	208.01 (<i>selected order</i>)
Trend Surface (3 rd order)	434.83
Universal Kriging	157.09

5.6.2.3 Histogram Analysis of Lower Goru

Total data points for Lower Goru in XYZ data are 396 with mean value 1633.6. In case of XYZ data most of the data points are clustered near the mean value as shown in Fig 5.15(A). In filtered XYZ data large values are filtered out which are affecting the mean value as shown in Fig 5.15(B). After filtering number of data points for Lower Goru reduced to 340.

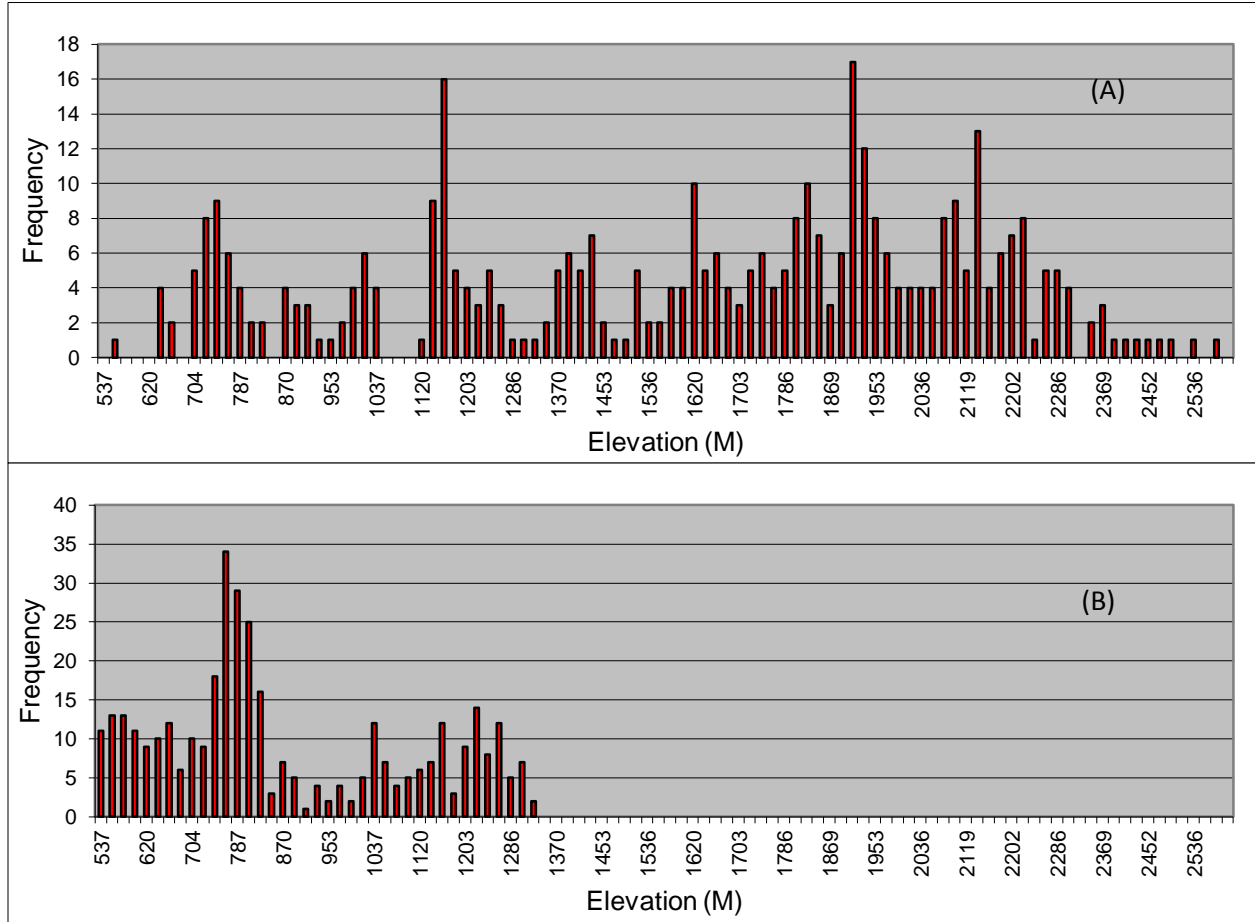


Fig 5.15: Histograms of XYZ (A) and XYZ filtered data (B) of Lower Goru

5.6.2.3 3D Surfaces of Lower Goru

3D surfaces of Lower Goru are generated in the similar way as the previous formations. Surfaces show that the formation is dipping in NW direction. Ordinary Kriging gives the local geometric variations. 2nd order of Trend Surface passes as best fit, thus the equation is also derived for it. 2nd order surface shows some shallow structure towards east as shown in Fig 5.16. 2nd Order polynomial equation is;

$$Z_{L_Goru} = -8513257.15 + 267587.72 \lambda - 45319.63 \phi - 1944.45 \lambda^2 - 156.19 \lambda \phi + 1135.565 \phi^2 \quad \dots \dots \dots (5.7)$$

Universal Kriging surface gives the regional trend of formation by using all data points in computation of variogram. To model the regional trend along with prominent variations, a smoothing Kernel operator of 21*21 points is applied to Ordinary Kriging surfaces.

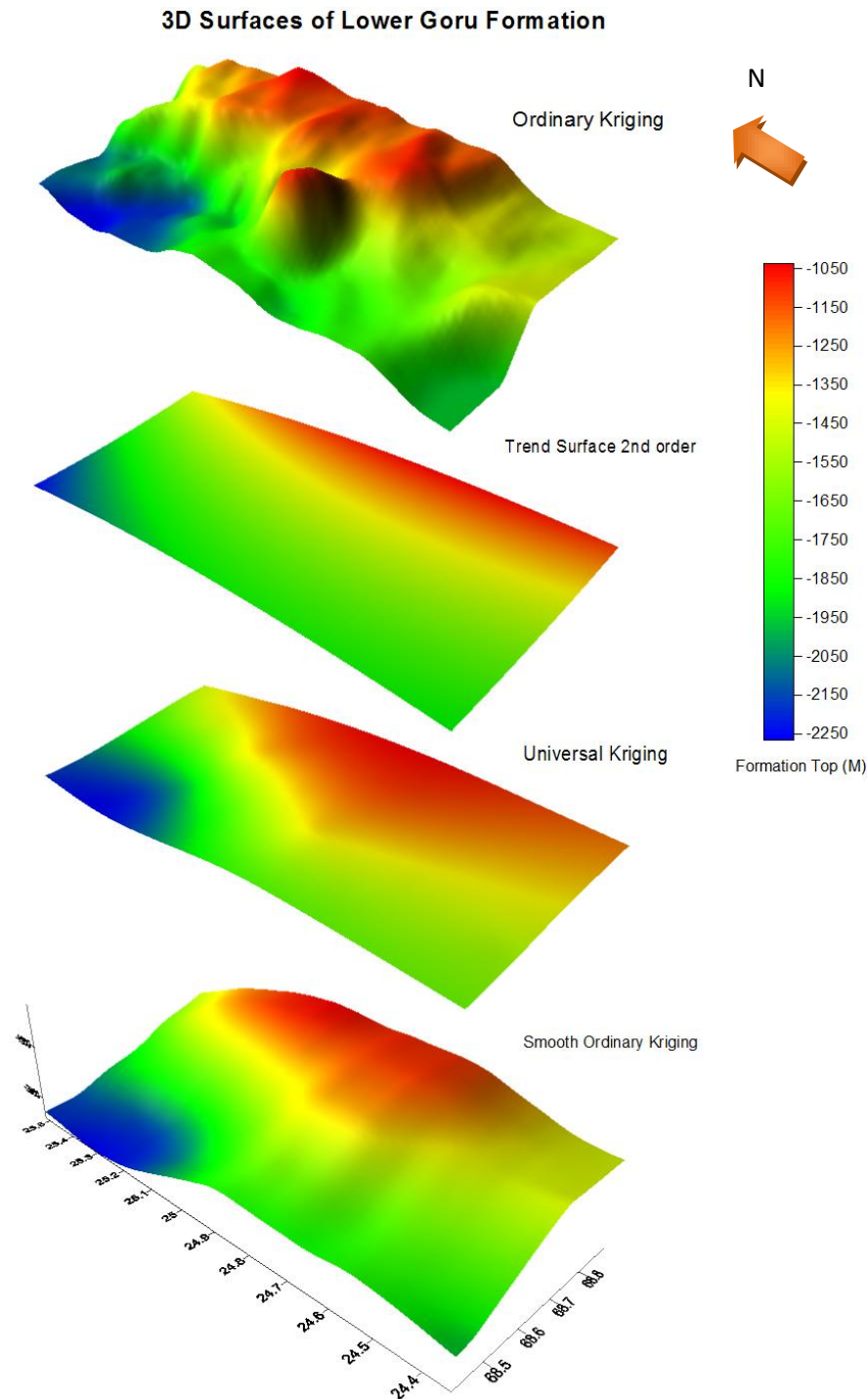


Fig 5.16: 3D surfaces of Lower Goru

5.7 Chiltan Formation

Chiltan Formation is mainly composed of limestone of Middle Jurassic age. General elevation of Chiltan varies from 2557.2 to 3932 meters. Mean top of Chiltan Formation is 3194 meters. 3D surfaces of Chiltan Formation are also generated using Ordinary Kriging, Trend Surfaces of 1st, 2nd order and then by Universal Kriging. Ordinary Kriging gives true picture of geometric variations of formation mean while 1st and 2nd order of Trend Surfaces and Universal Kriging model the regional trend. Then by applying 21*21 points smoothing operator on Ordinary Kriging, it is converted into a surface (Smooth Ordinary Kriging), which represents the regional trend and prominent local variations.

5.7.1 Statistical Analysis of Chiltan Formation

Selection of final surface depends on value of standard deviation. The value of standard deviation is decreases by increasing the order of Trend Surface as shown in Table 17. In case of Universal Kriging standard deviation reduced to 31.51. Thus Universal Kriging surface will give the regional trend of formation top of Chiltan Limestone. Standard deviation value is 430.84 in XYZ data, but by applying Standard Deviation Filter value of standard deviation decreased to 318.99. Statistical analysis of Chiltan Formation is given shown in Table 17.

Table 17: Statistical Analysis of Chiltan Formation

Data	N	Min	Max	Mean	Std Dev	Variance
XYZ	18	2557.15	3932	3194.04	430.84	185624.9
XYZ-Filtered	15	2557.15	3737	3052.08	318.99	101756.8
Ordinary Kriging	3600	2856.612	3182.2	3046.13	99.59	9919.47
Trend Surface 1	3600	2588.093	3655.25	3121.67	231.12	53417.69
Trend Surface 2	3600	2512.645	3680.41	3076.57	226.24	51184.53
Universal Kriging	3600	3006.94	3127.85	3064.94	31.51	992.93

5.7.2 Standard Error of Chiltan Formation

Standard error of Chiltan Formation for Trend Surface of 1st order is 163.54, for 2nd order is 156.12 and then it reached to 694.02 for 3rd order. Thus 2nd order grid is selected. Standard error is 65.18 in case of Universal Kriging, which is smaller than Trend Surface (increasing orders) shown in Table 18.

Table18: Standard Error of Chiltan Formation

Grid	Standard Error
Trend Surface (1 st order)	163.54
Trend Surface (2 nd order)	156.12 (selected order)
Trend Surface (3 rd order)	694.02
Universal Kriging	65.18

5.7.3 Histogram Analysis of Chiltan

In case of Chiltan Formation 18 total data points were found in XYZ data having mean value 3194.039. Data points which are producing large fluctuations are removed and the mean value reduced to 3052.081. Histograms of XYZ and XYZ Filtered data are shown in Fig 5.17(A, B).

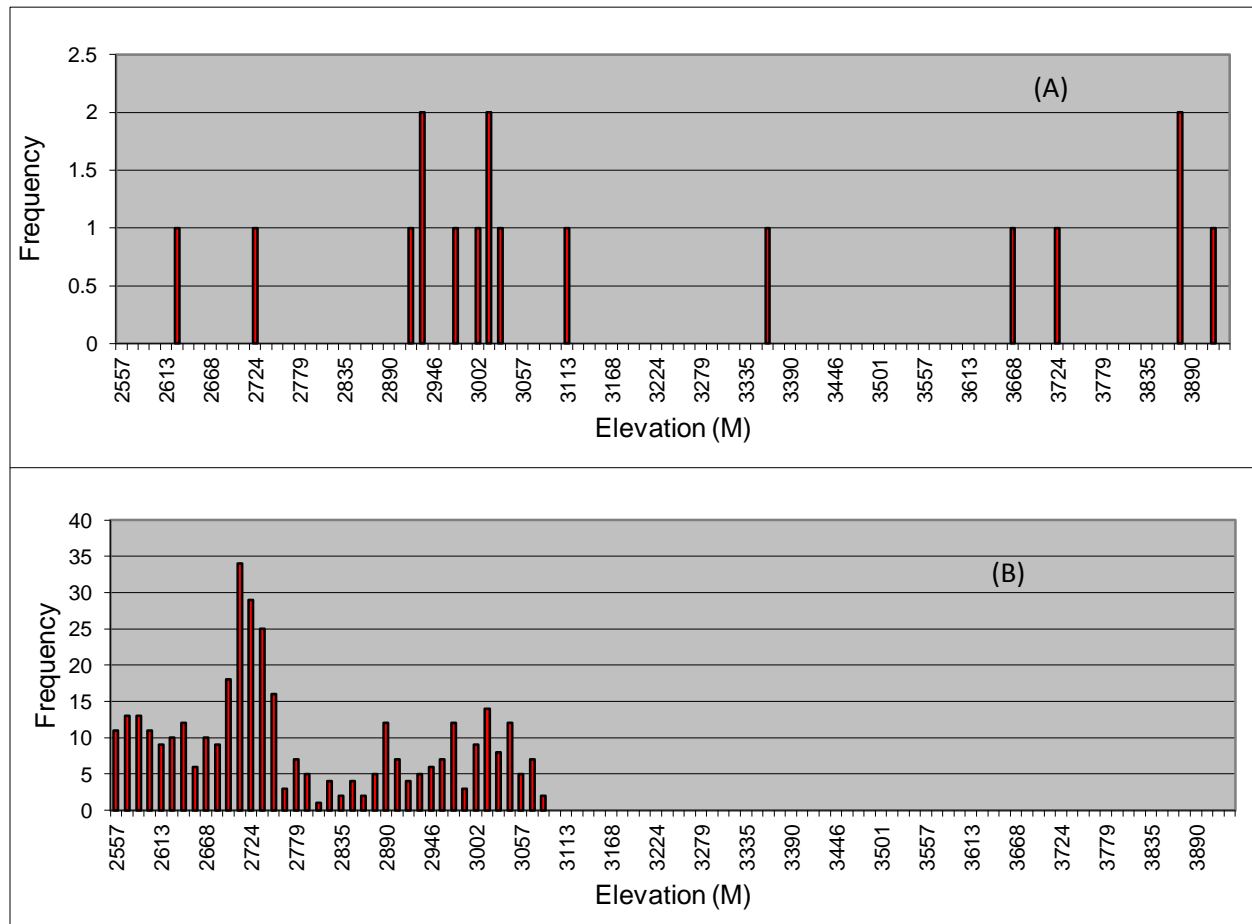


Fig 5.17: Histograms of XYZ (A) and XYZ filtered data (B) of Chiltan Formation

5.7.4 3D surfaces of Chiltan Formation

Based on the results of statistical analysis and standard error values, 3D surfaces of Chiltan are generated by Ordinary Kriging, Trend Surface of 3rd order and then by Universal Kriging as shown in Fig 5.18. General gradient of the formation is from north to south. Ordinary Kriging gives the local geometric variations and showing strong N-S gradient. It shows that north eastern and south eastern part of formation is at greater depths. 2nd order of surface have single flexure along with plane and shows the regional trend of Chiltan Formation that is NS. 2nd Order polynomial equation is;

$$Z_{Chiltan} = 4820937.573 - 221015.388\lambda + 219882.703\phi + 1968.643\lambda^2 - 1949.426\lambda\phi - 1728.878\phi^2$$

Universal Kriging surface gives the regional trend of formation by using all data points in computation of variogram. To model the regional trend along with prominent variations, a smoothing Kernel operator of 21*21 points is applied to Ordinary Kriging surfaces.

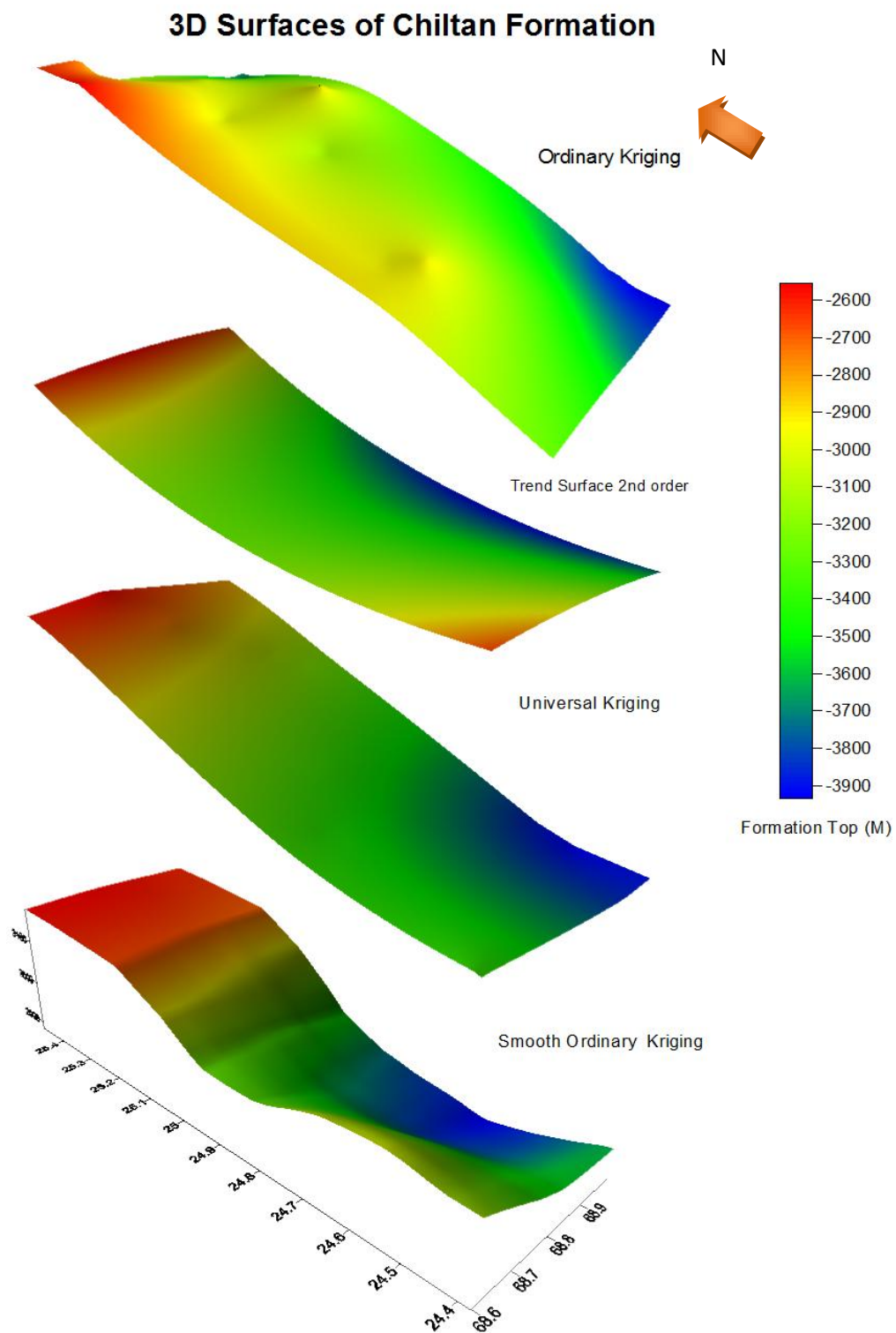


Fig 5.18: 3D surfaces of Chiltan Formation

Chapter 6 Digital Sub-Surface Model

6.1 Introduction

A Digital Elevation Model (**DEM**) is basically a 3D representation of topographic variations of any surface, which is created from elevation data of that area (Maune, 2007). The data is collected by remote sensing techniques or by land surveying to build DEM. DEM as a regularly spaced GRID and is very useful in geographic information system and provide a base for digital topographic maps. Whereas **Digital Sub-Surface Model (DSSM)** consists on multiple grids as there are multiple layers are present in subsurface. Conventionally the surface grids are used to generate the contour map or 3D surface for visualization. K-tron GridWorks is a DSSM technology used to create the subsurface model of the area by integrating all the surfaces. The advantage of this technique is that we can interactively generate 1D subsurface columns and 2D cross sections that can be helpful in geological analysis and seismic interpretation.

6.2 Development of Digital Sub Surface Model

DSSM is developed with the help of Microsoft Visual Basic and K-tron GeoStudio. Following is the list of libraries which are used;

1. GeoStat (Statistical Analysis)
2. GridPro (Gridding, Smoothing)
3. Geometry (Geometric problems)
4. GeoLIB (Export columns and cross sections to display in X-Works).

6.3 Software Application

The interface of GridWorks: Digital Sub-Surface Model application is shown in Fig 6.1. All the subsurface grids generated in previous chapter are integrated by this software tool.

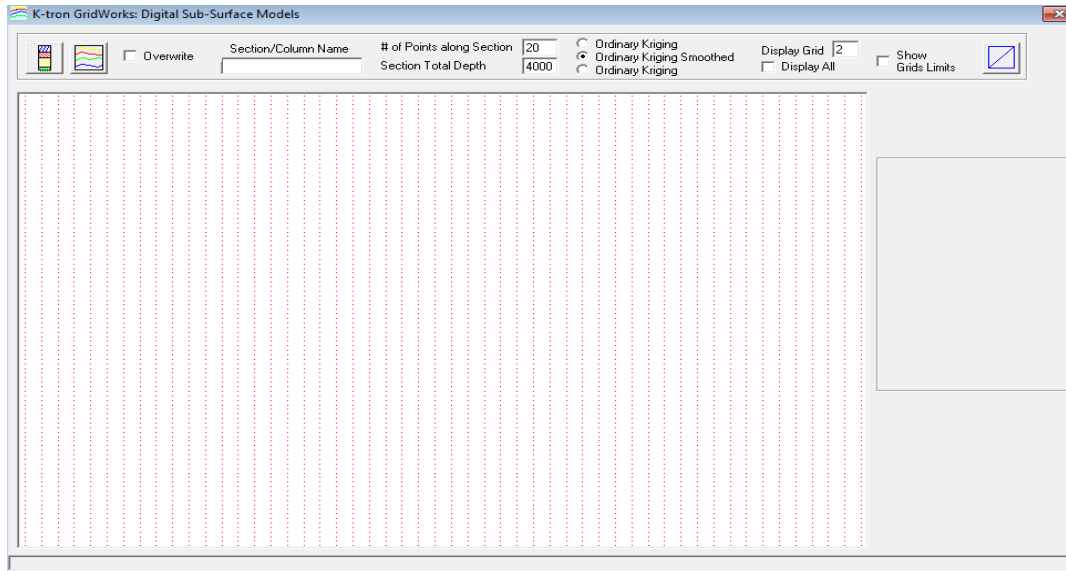


Fig 6.1: The interface of GridWorks: Digital Sub-Surface Model application

In addition the software allows creation of models on different types of grids such as an order of trend surface, Ordinary Kriging or its smoothed version. Currently three types of grids are used to generate digital sun-surface model.

1. Ordinary Kriging
2. Smooth Ordinary Kriging
3. Universal Kriging

The workflow of this system such as generation of 1D column and 2D cross-sections is shown in Fig 6.2.

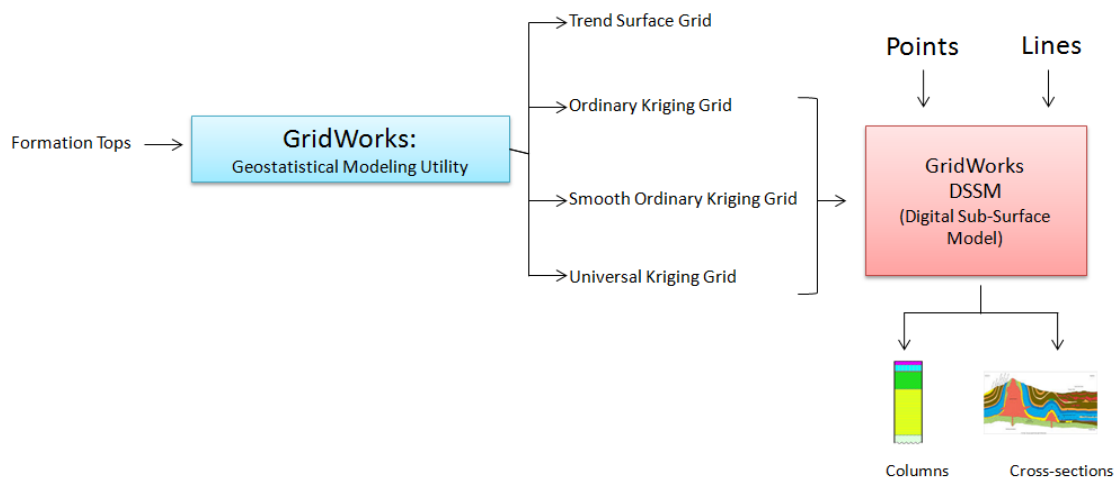


Fig 6.2: Workflow of Columns and Cross-Section generation

The system provides an interactive interface through which points or lines are marked to generate geological columns and cross-sections respectively. The columns and cross-section data can be saved in K-tron X-Works COL and Sec formats respectively, which in turn displays them for visualization. Fig 6.3 shows a column generated by the system.

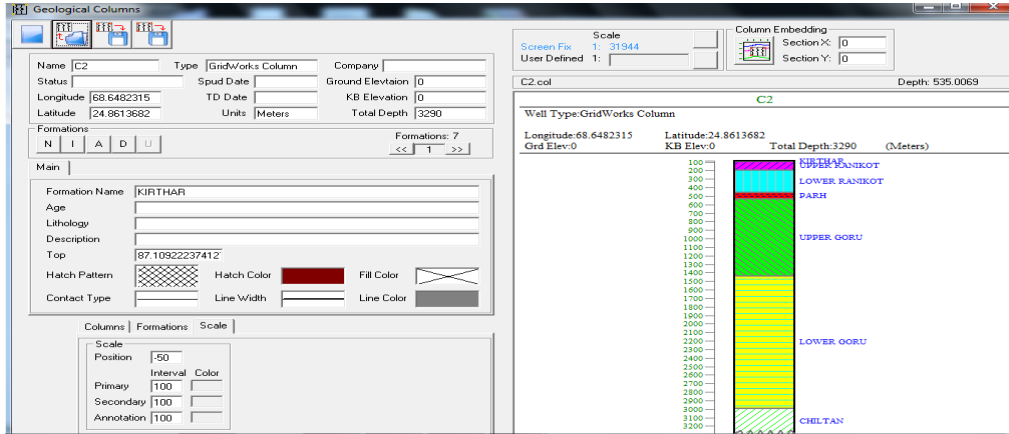


Fig 6.3: Column generation at any spatial location

To extract the formation data at any spatial location from the Digital Sub-Surface Model (DSSM), the software uses bilinear interpolation which is discussed in next section.

6.4 Bilinear Interpolation

Generally bilinear and bicubic interpolation techniques are used to interpolate the data at any point from a gridded dataset. Bicubic interpolation uses 4*4 grid operators of sixteen grid nodes around the interpolation point. Bilinear interpolation uses 2*2 grid operators of four grid nodes around the interpolation point. Bicubic interpolation is compute intensive, but produces a smoothed effect .Since our input grid have already smoothed therefore bilinear interpolation is preferred on bicubic interpolation.

Bilinear interpolation is an interpolation technique used to interpolate functions of two variables (x and y) on a 2D grid. The rule behind this quadratic interpolation is that, first linear interpolation will be performed in one direction and then again in the other direction. If we are interested to find the value of f at any particular location (x, y) , we have to assume that we know the value of f at the four locations $Q_{11} = (x_1, y_1)$, $Q_{12} = (x_1, y_2)$, $Q_{21} = (x_2, y_1)$, and $Q_{22} = (x_2, y_2)$ as shown in Fig 6.4. Thus first we do linear interpolation in the x -direction, which yields;

$$f(x, y_1) \approx \frac{x_2 - x}{x_2 - x_1} f(Q_{11}) + \frac{x - x_1}{x_2 - x_1} f(Q_{21})$$

$$f(x, y_2) \approx \frac{x_2 - x}{x_2 - x_1} f(Q_{12}) + \frac{x - x_1}{x_2 - x_1} f(Q_{22})$$

Then we will continue by interpolating in the y-direction,

$$f(x, y) \approx \frac{y_2 - y}{y_2 - y_1} f(x, y_1) + \frac{y - y_1}{y_2 - y_1} f(x, y_2)$$

$$\approx \frac{y_2 - y}{y_2 - y_1} \left(\frac{x_2 - x}{x_2 - x_1} f(Q_{11}) + \frac{x - x_1}{x_2 - x_1} f(Q_{21}) \right) + \frac{y - y_1}{y_2 - y_1} \left(\frac{x_2 - x}{x_2 - x_1} f(Q_{12}) + \frac{x - x_1}{x_2 - x_1} f(Q_{22}) \right)$$

$$= \frac{1}{(x_2 - x_1)(y_2 - y_1)} (f(Q_{11})(x_2 - x)(y_2 - y) + f(Q_{21})(x - x_1)(y_2 - y) + f(Q_{12})(x_2 - x)(y - y_1) + f(Q_{22})(x - x_1)(y - y_1))$$

The data points are represented by four red dots and “P” is the green dot at which we are interested to interpolate.

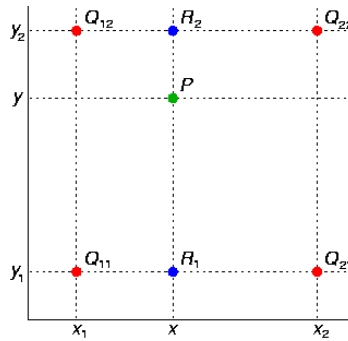


Fig 6.4: Linear Interpolation at point P

6.5 Practical Application

As all the geologic formations may not exist at each location within the area, therefore grid generate for the entire formations lie within the different geological limits. However all the grids have an overlapping area, where all the formations are present within that area. The software shows all the individual grid nodes for a formation as well as grid nodes for all formations as shown in the Fig 6.5 and Fig 6.6 respectively.

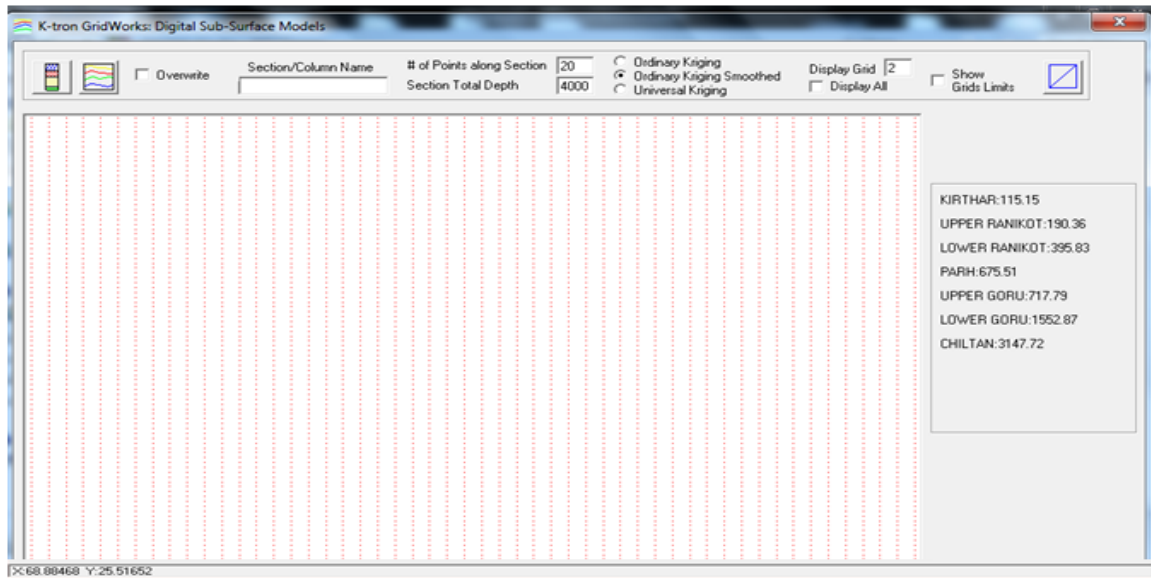


Fig 6.5: Individual Grid Nodes of Upper Ranikot Formation

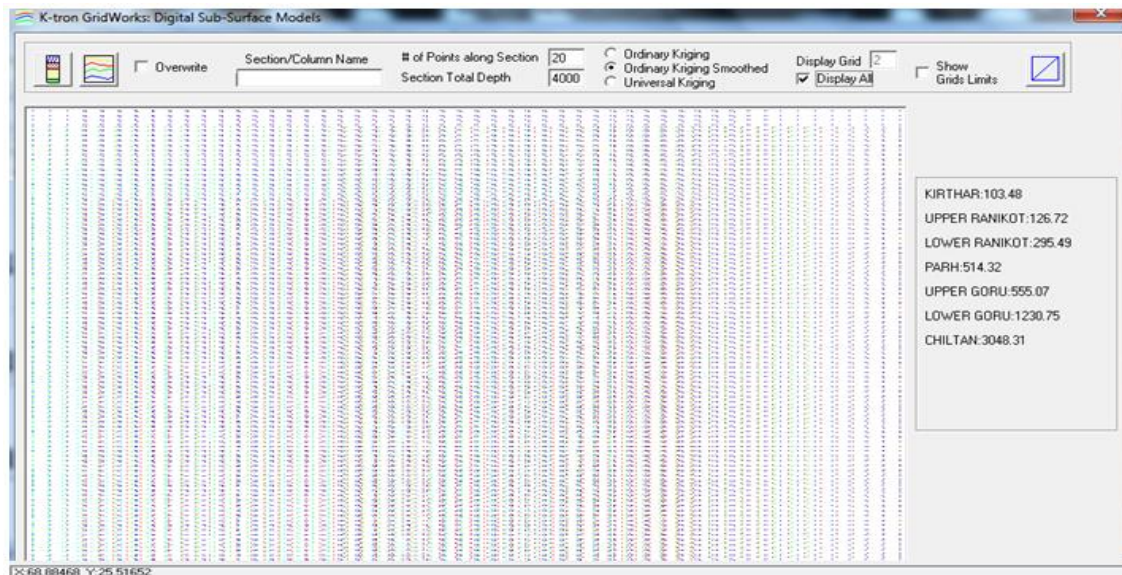


Fig 6.6: Grid nodes for all formations central part is overlapping zone

The software provides a highly interactive interface. Simply moving mouse at any point on the map shows its latitude-longitude position and the formation tops information below that point as shown in Fig 6.7. By pointing C8 having geographic coordinates X (68.88468) and Y (25.51652), all the formations lying beneath that point and their average top can be seen on the right side of interface.

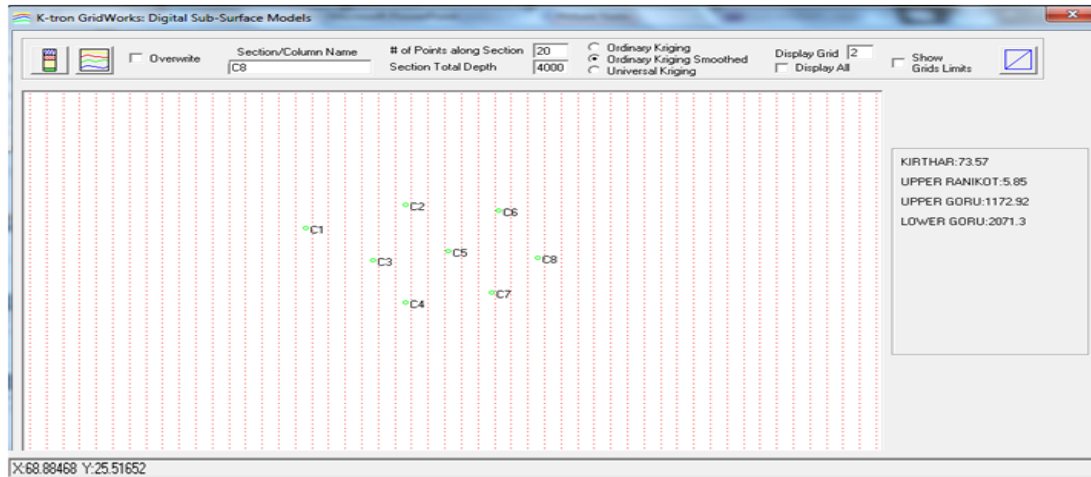


Fig 6.7: Selection of spatial location and all formations present beneath that point

Using the column export function columns at various points of interest can be generated and can be saved in K-tron X-Works Col format. Fig 6.8 shows the software used for column generation and Fig 6.9 shows the columns generated by X-Works for these points.

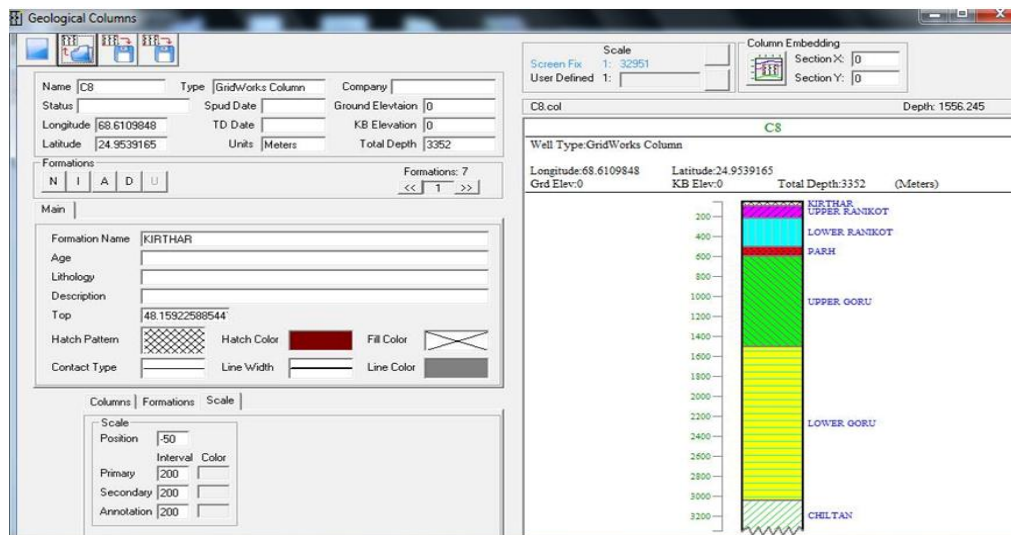


Fig 6.8: Generation of 1D column at geographic location C8

Here we marked eight points i.e. eight spatial locations from C1 to C8 on the grid, the columns generated for these locations are shown in Fig. 6.9 containing all the formations which are encountered at those eight locations. Thickness variations of Parh can be seen through eight spatial positions. It is thicker in columns generated at C2, C5 and C8 and comparatively at C7 locations. Parh is very thin in columns generated at spatial locations C1, C3 and C4.

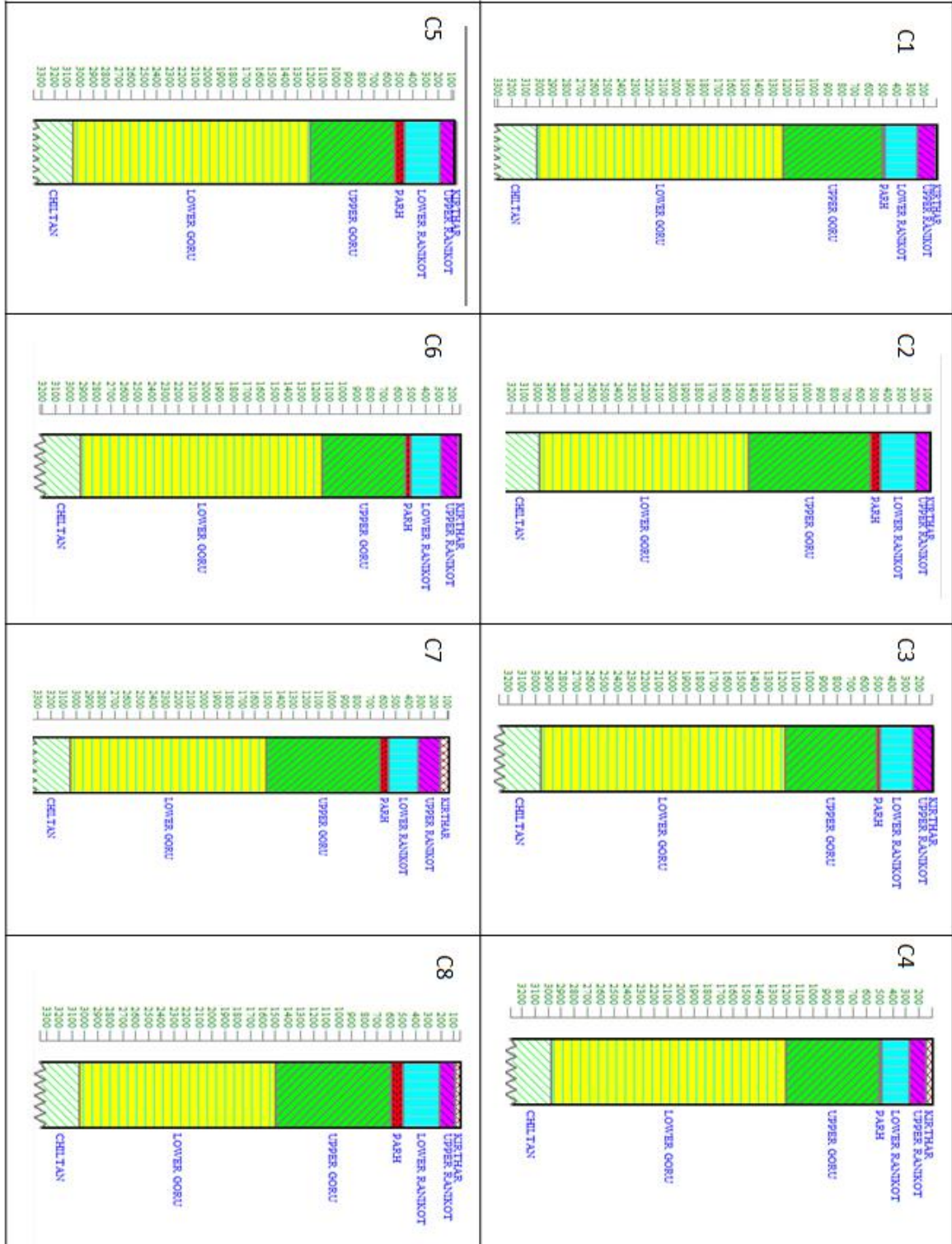


Fig. 6.9: Columns generated for eight locations (C1-C8) along all the encountered formations

In addition to columns the software also generates cross sections along the lines which can be interactively drawn on the map. The software also provides option for selection number of data points to be interpolated between line ends. The selected formations data along the line can be interpolated to X-works for display. Fig 6.10 shows the software interface with interactively marked lines and Fig 6.11 shows the cross section generated by these line S1 having all modeled formations and X-axis is the distance in meters and y-axis is the depth in meters. Fig 6.12 to Fig 6.15 shows the cross sections generated by these lines (S2-S5). Upper Ranikot and Parh are pinching out at some locations shown in figures below.

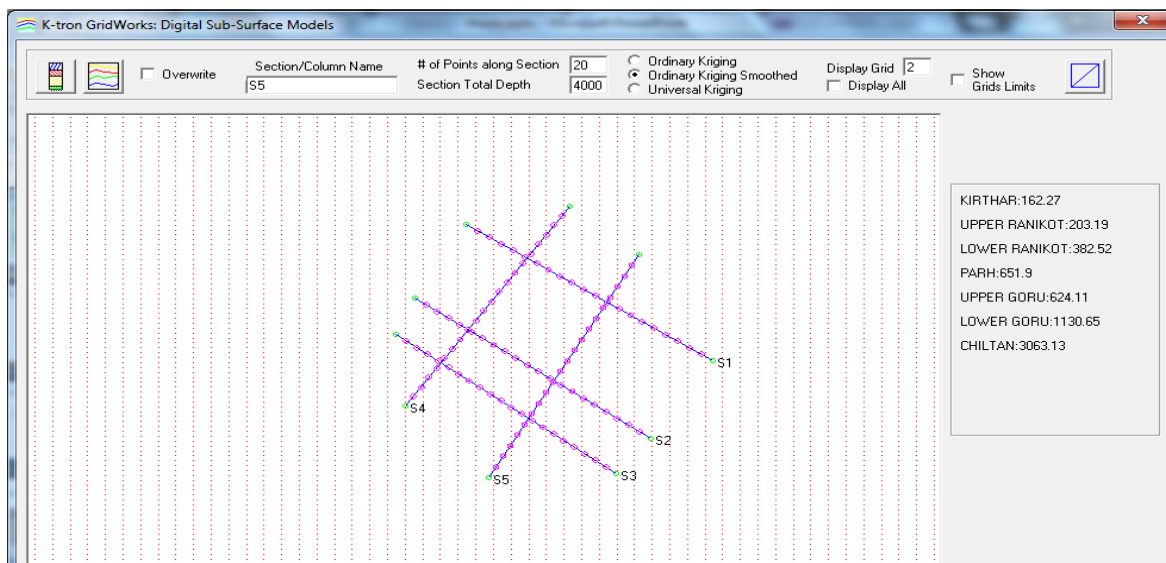


Fig 6.10: DSSM which interactively marked lines

Digital sub surface cross sections are generated along different lines having different orientations, than forward modeling is carried out at those lines which will be helpful in estimating seismic parameters for a new survey. Digital sub surface cross section of line S1 is given in Fig 6.11.

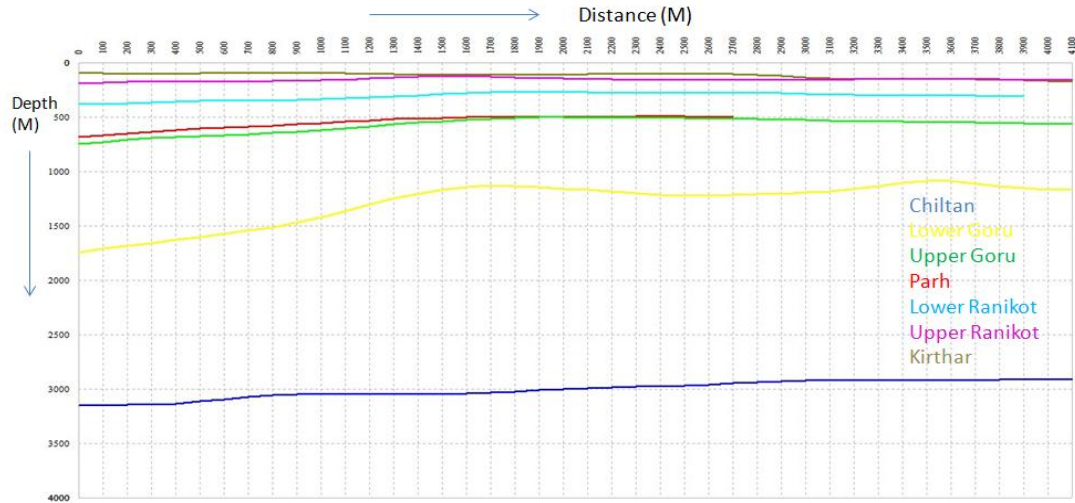


Fig 6.11 The cross section generated from line S1

6.5 2D synthetic seismic model

To get the seismic response of selected formations, 2D synthetic seismic model is generated. It is helpful in seismic structural interpretation and in selection of acquisition parameters i.e. frequency and resolution for new survey. More the frequency more will be resolution and the thin beds can easily be resolved. As in seismic surveys we are interested in deep horizons so frequency is small and more will be penetration. To generate 2D synthetic model a synthetic source wavelet Ricker is generated having dominant frequency of 35Hz and signal to noise ratio 3 and velocity of basin is used. The synthetic seismic model exactly matched all digital sub surface models generated. 2D synthetic seismic model of Digital Sub-Surface Model S1 is shown in Fig 6.12.

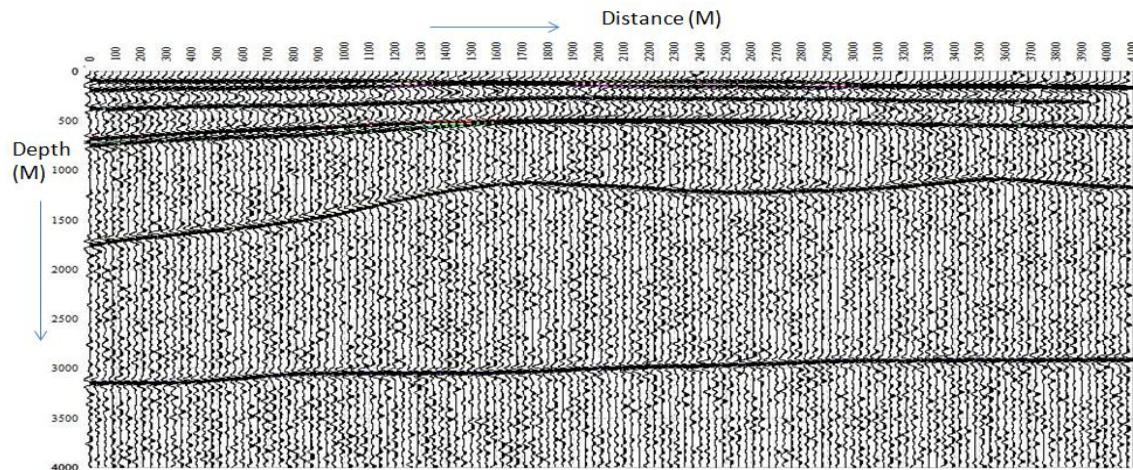


Fig 6.12: 2D Synthetic Seismic Model of S1

On the similar way cross sections and 2D forward modeling is carried out along different lines given as under.

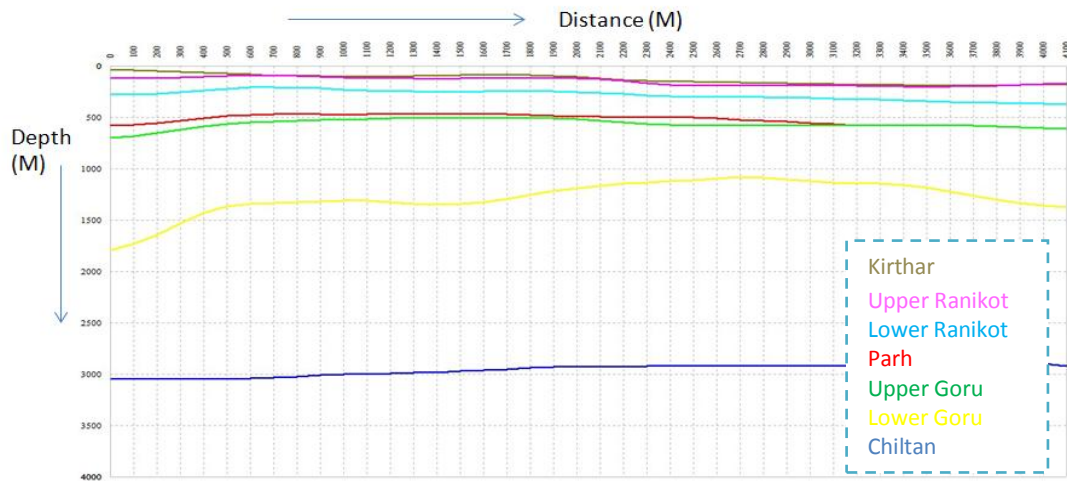


Fig 6.13: The cross section generated from line S2

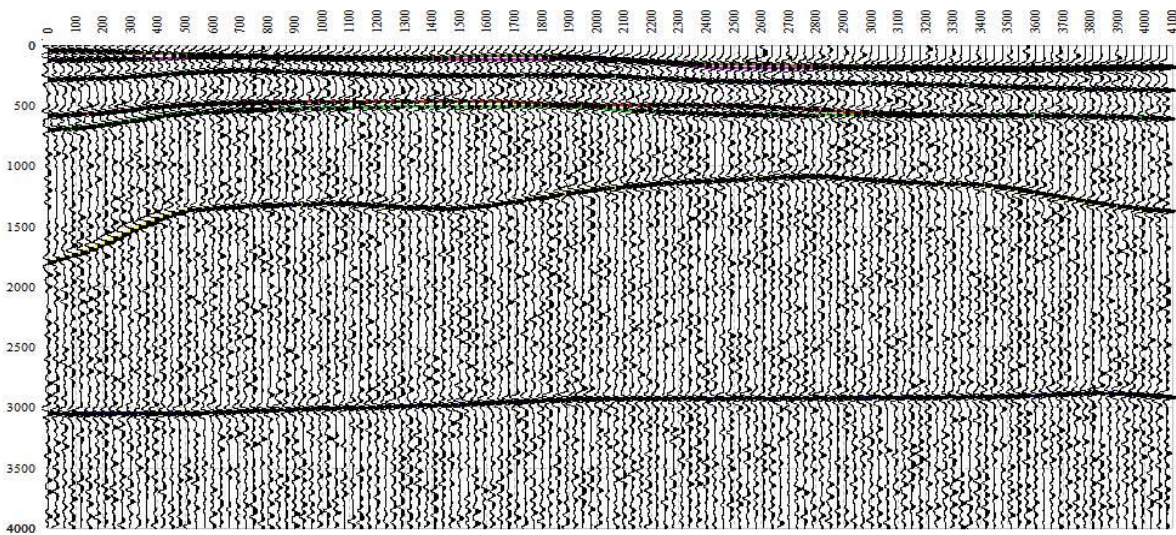


Fig 6.14: 2D Synthetic Seismic Model of S2

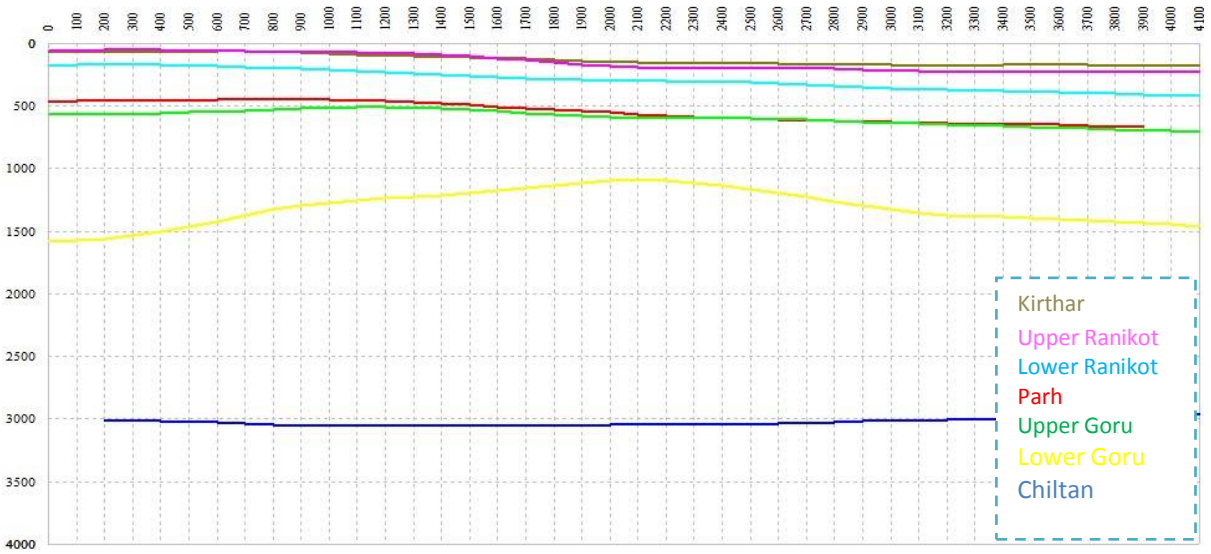


Fig 6.15: The cross section generated from line S3

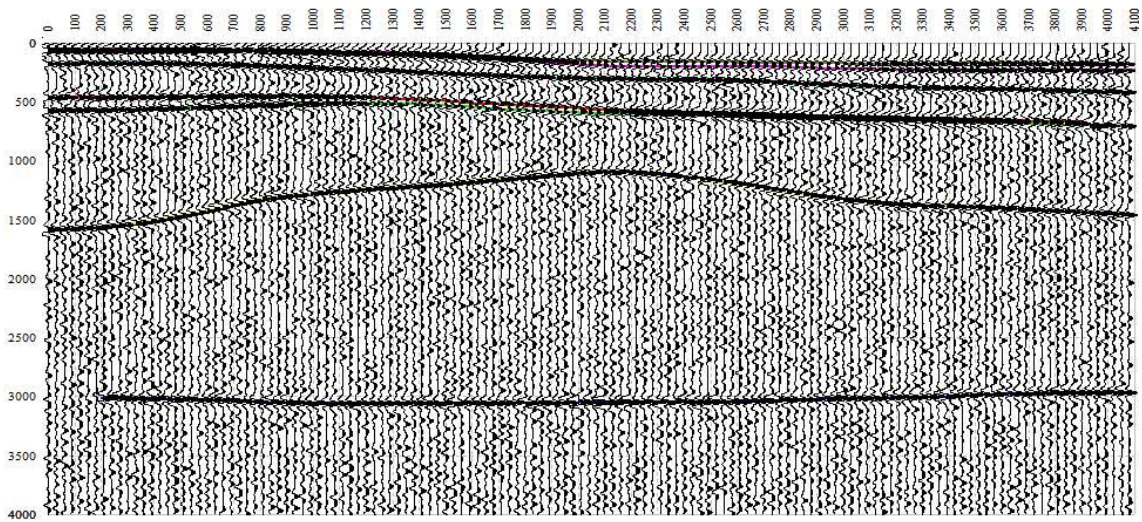


Fig 6.16: 2D Synthetic Seismic Model of S3

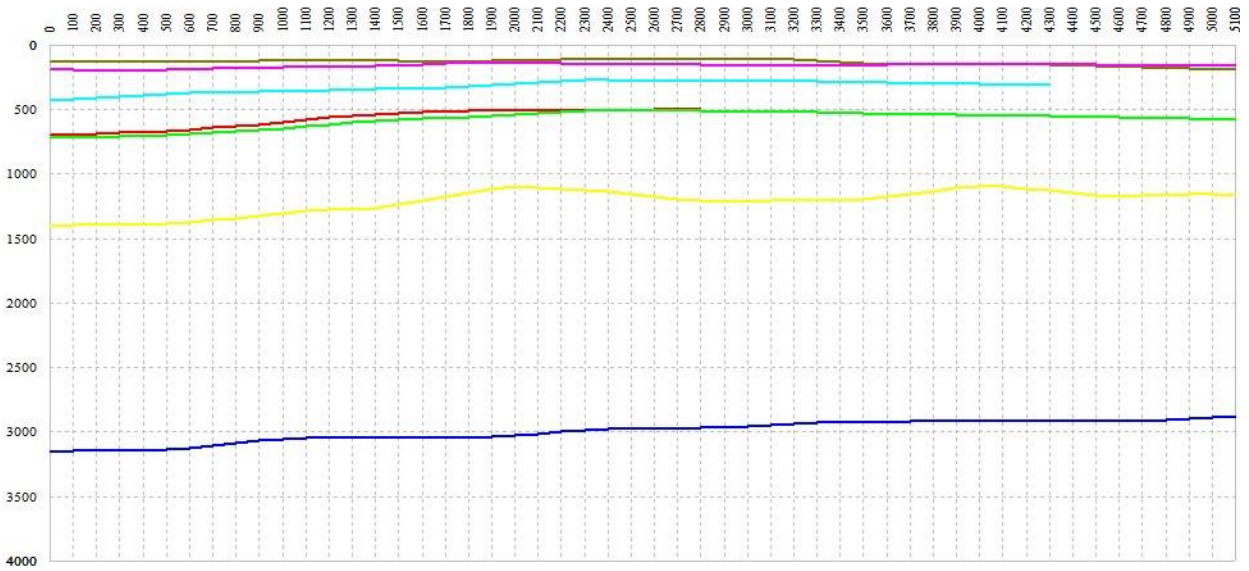


Fig 6.17: The cross section generated from line S4

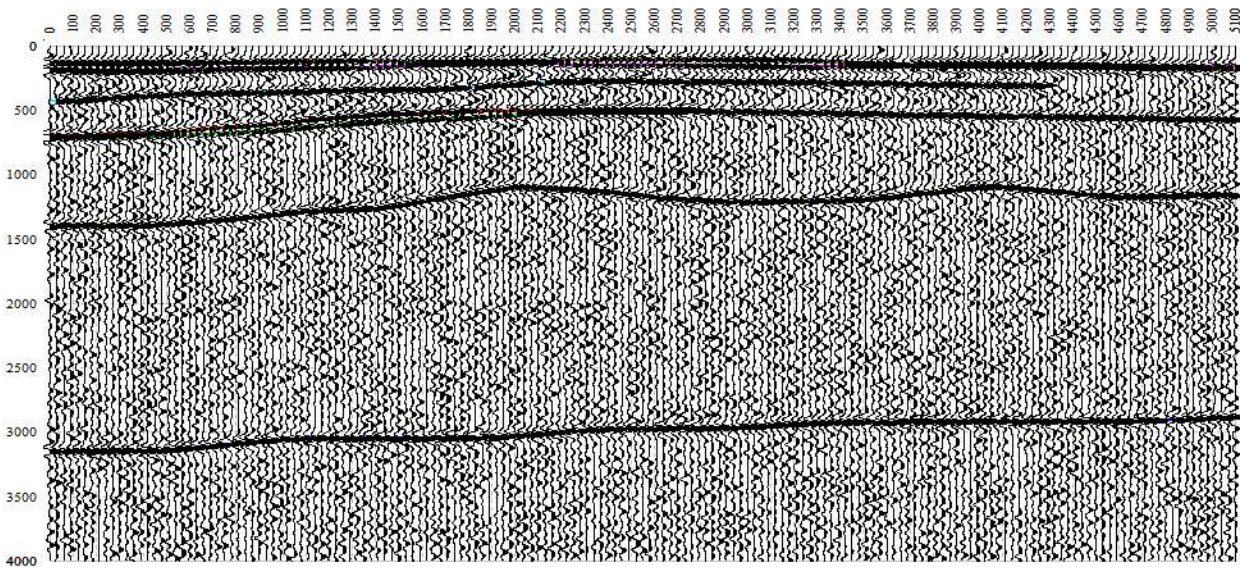


Fig 6.18: 2D Synthetic Seismic Model of S4

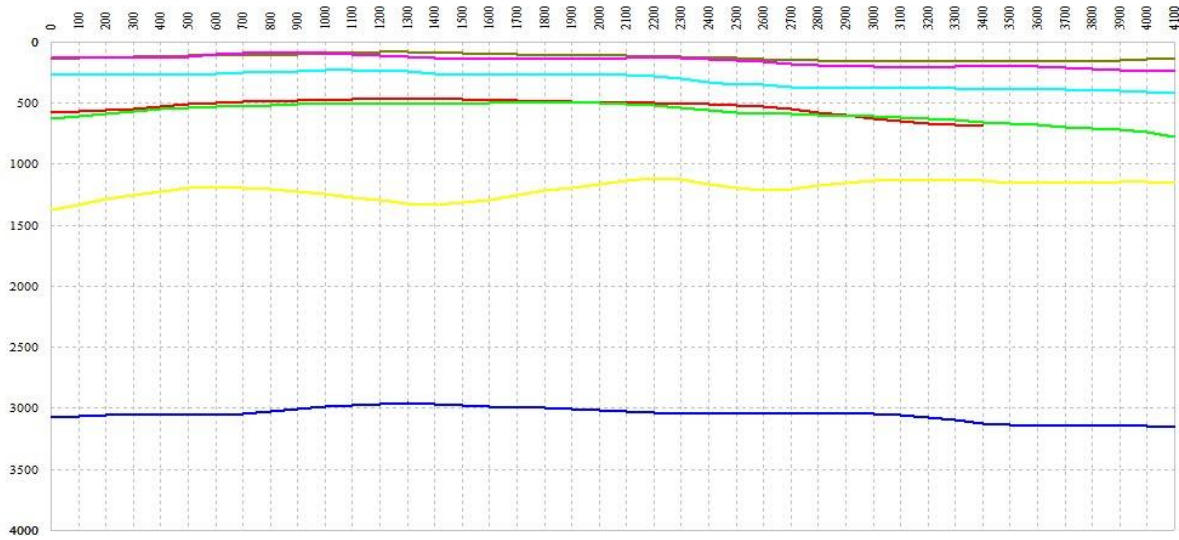


Fig 6.19: The cross section generated from line S5

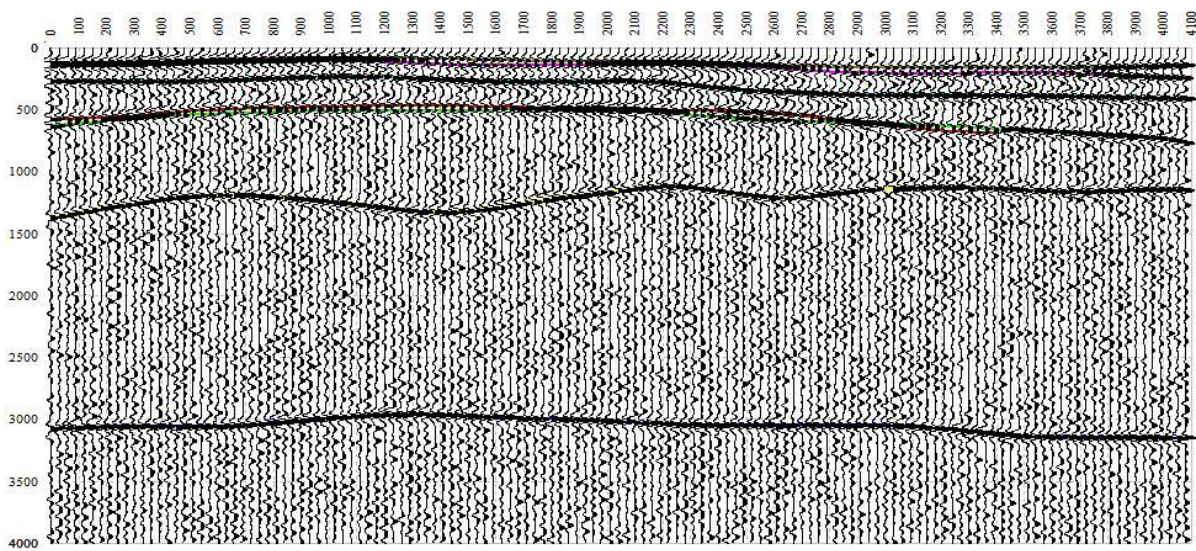


Fig 6.20 2D Synthetic Seismic Model of S5

These subsurface geological cross sections are helpful to determine the seismic acquisition parameters for new seismic survey. 2D synthetic seismic model can also be generated from these geological sections. The 2D synthetic seismic models for all digital sub surface sections are generated. These 2D synthetic models exactly match all digital sub surface models, which is the confirmation of our sub surface model of selected formations of Lower Indus basin.

6.6 Seismic Line PK-92

Digital sub Surface Model (DSSM) of Lower Indus basin can be useful in seismic interpretation of adjacent areas, establishing well control over a point and generation of correlation profiles. Seismic line PK-92 Fig 6.21 is interpreted with the help of Digital sub Surface Model of Lower Indus basin. Time section is converted into depth section by using the velocity information of basin.

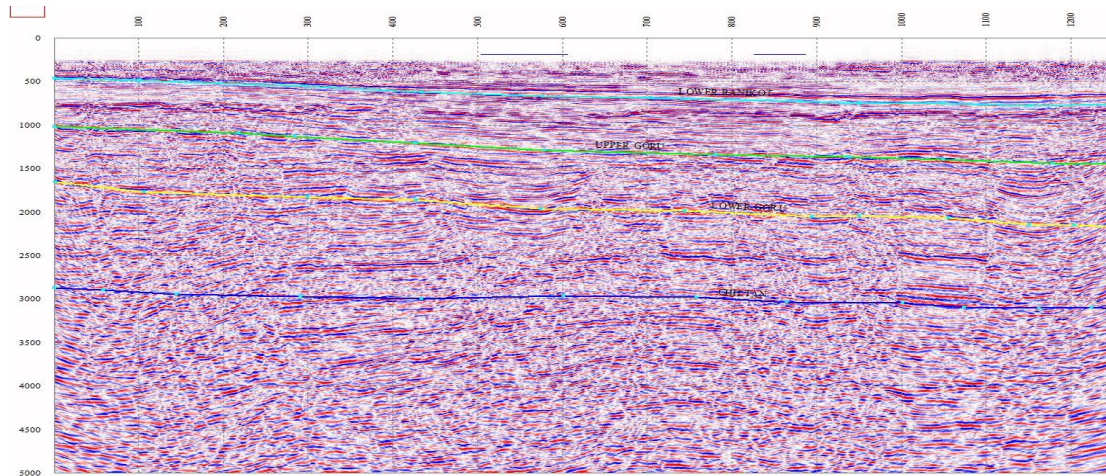


Fig 6.21 Interpreted PK-92 with Digital sub Surface Model.

By analyzing the zoomed image after interpretation of seismic line as shown in Fig 6.22, it is found that the interpretation is not exactly along the reflectors but it gives generalized interpretation and does not follow the reflectors in detail.

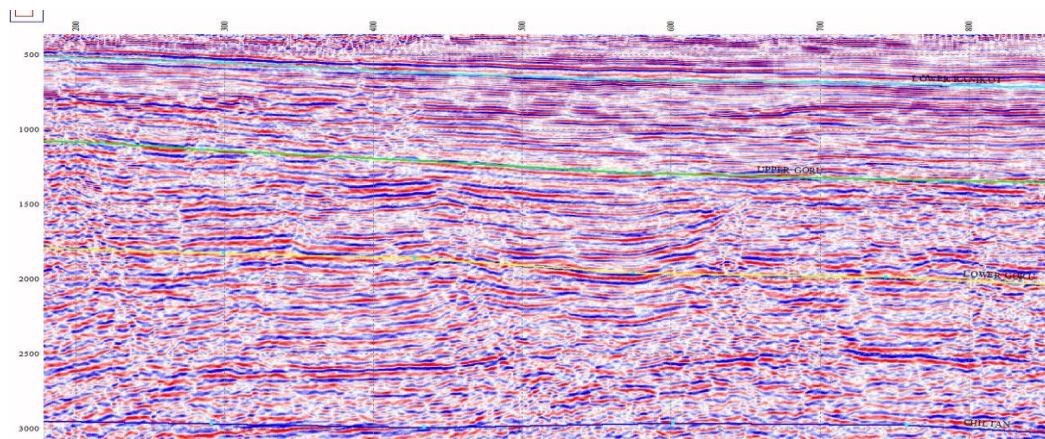


Fig 6.22 Interpreted PK-92 with Digital sub Surface Model zoomed section

Conclusion and Recommendations

Conclusions

1. Geostatistical modeling of various formations in Lower Indus Basin was carried out by using formation tops data of 461 wells.
2. Second and third order trend surface provide a generalized best fit through the data. In the absence of any data the resulting equations can be used to get a rough idea about the formations at any given location.
3. Geological surface have been generated by using different Geostatistical techniques. It has been found that smoothed ordinary Kriging provides subsurface model with reasonable local details, while universal Kriging provide more generalized trend.
4. The Geostatistical grids are used to assemble a multilayer Digital Sub-Surface Model (DSSM) which can be used to generate columns and subsurface cross-sections within the area. This can be useful in seismic interpretation of adjacent areas, establishing well control over a point and generation of correlation profiles.
5. The subsurface geological cross sections are helpful to determine the seismic acquisition parameters for new seismic survey.

Recommendations

1. In Geostatistical mapping selection of surfaces is based on values of standard error and standard deviation, but it can be done with the help of F-test.
2. To analyze the general gradient of formations Universal Kriging technique will give best results.
3. To analyze the subsurface model with local details such as high and lows, Ordinary Kriging is suggested.

References

- Agarwal, R.G., Kanasevich, E.R., 1971, Automated trend analysis and interpretation of potential field data. *Geophysics*, vol. 36, P.339-348.
- Chiles, P.J., and Delfiner, P., 1999, First Edition, *Geostatistics Modeling Spatial Uncertainty*.
- Chiles, P.J., and Delfiner, P., 2012, Second Edition, *Geostatistics Modeling Spatial Uncertainty*.
- Cressie, N., 1985, Fitting Variogram by weight least square, *Journal of International Association of Mathematical Geology* 17, 563-586.
- Hengl, T., 2011, *A Practical Guide to Geostatistical Mapping*.
- Kadri, I.B, 1995, *Petroleum Geology of Pakistan*, PPL Pakistan.
- Kazmi, A.H, and Jan, M.Q, 1995, *Geology and Tectonics of Pakistan*, Graphic publishers, Karachi, Pakistan.
- Kazmi, A.H, and Jan, M.Q, 1997, *Geology and Tectonics of Pakistan*, Graphic publishers, Karachi, Pakistan.
- Kemal, A., Balkwill, H. R. and Stoakes, F.A., 1991 , *Indus Basin Hydrocarbon Plays, International Petroleum Seminar on New Directions and Strategies for Accelerating Petroleum Exploration and Production in Pakistan* , P.16-57.
- Khan, K.A., 2000, *Integrated Geo Systems - A Computational Environment for Integrated Management, Analysis And Presentation Of Petroleum Industry Data*, In: T. C. Coburn And J. M Yarus (Eds.), *Geographic Information Systems In Petroleum Exploration And Development*, AAPG Book on Computers and Geology, P.215-226.
- Khan, K.A., 2014, *Manual of Geostatistics for Geoscientists and Reservoir Engineers*, OIST, Islamabad.
- Khan, K.A., Akhter, G., and Ahmad, Z., 2010, *OIL - Output Input Language for Data Connectivity between Geoscientific Software Applications*, Computers & Geosciences.

- Khan, K.A., Akhter, G., and Ahmad, Z., and Rashid, M., 2008, Development of a Projection Independent Multi-Resolution Imagery Tiles Architecture for compiling an Image database of Pakistan, Proceedings of 2nd International Conference on Advances in Space Technologies Islamabad, Pakistan, P.164-170.
- Maune, F. D., American Society for Photogrammetry and Remote Sensing, 2007, Technology & Engineering, P. 655.
- Merriam, D.F., Harbaugh, J.W., 1963, Computer helps map oil structures. Oil and Gas Journal 61, P.158–163.
- Merriam, D.F., Lippert, R.H., 1966, Geologic model studies using trend-surfaces analysis. Journal of Geology 74, P.344–357.
- Powell, C.M., and Conaghan, P.J. 1973, Plate tectonics and the Himalayas. Earth and Planetary Science Letters, P.687-697.
- Roger, K., 2005, Quantile Regression, Cambridge University Press, United Kingdom.
- Zaigham, N.A, and Mallick, K.A, 2000, Prospect of hydrocarbon associated with fossil-rift structures of the southern Indus basin, Pakistan, American Association of Petroleum Geologists Bulletin.

Appendix 1

```
;WellRecFT - Search Formation Tops from Wells Records File
;Nosheen Akhtar    08.02.2015  01.00
protocol Nill
tunnel Nill
help Search Formation Tops from Wells Records Fil
help
help Searches the given Formation Top from Wells Records File and outputs the data as an XYZ File
help
help User Parameters
help * Input Well Records File [\igs\dat\report]
help * Formation Name
help * Output Well Records File [\igs\dat\report]

dispdata /Search Formation Tops from Wells Records File/

                                ;get user parameters
dispdata /Enter Input Wells Records File [.TXT]/
userin a51
;$open:Well Records File,\igs\dat\report.txt
set a51 = a51 + /\.txt
pathfile /\igs\dat\txt\ a51 a51
dispdata /Enter Formation Name/
userin a52
dispdata /Enter Output XYZ File [.DAT]/
userin a53
;$save:XYZ Formation Tops Data,\igs\dat\xyz.dat
set a53 = a53 + /\.dat
pathfile /\igs\dat\xyz\ a53 a53

fileopen a51 i 1                ;open input well records file
fileopen a53 o 2                ;open output well records file

clear

start

getdata 1
scandata a52 n80
if n80 > 0                      ;if formation found
if n80 < 133
    count n81 ++ 1
    math n40 = 0
    xtrcdata 1 20 a1
    xtrcdata 21 30 n1           ;get longitude
    xtrcdata 31 40 n2           ;get latitude
    xtrcdata 114 158 a11
    xtrcdata 159 167 n11
    dispdata a1 a11 n1 n2 n11
endif
end

color 15                      ;display end message
```

```
dispdata //
dispdata / Search Completed/
if n81 = 0
    dispdata / No Records found./
endif
if n81 > 0
    dispdata n81 /Records Found./
endif
```